

# **-Model Predictive Control Based Wind-Solar Hybrid Energy Conversion System-**

Nikhil Bhugra

A Dissertation Submitted to  
Indian Institute of Technology Hyderabad  
In Partial Fulfillment of the Requirements for  
The Degree of Master of Technology



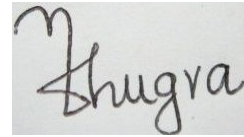
भारतीय प्रौद्योगिकी संस्थान हैदराबाद  
Indian Institute of Technology Hyderabad

Department of Electrical Engineering

June, 2013

## Declaration

I declare that this written submission represents my ideas in my own words and where others' ideas or words have been included, I have adequately cited and referenced the original sources. I also declare that I have adhered to all principles of academic honesty and integrity and have not misrepresented or fabricated or falsified any idea/data/fact/source in my submission. I understand that any violation of the above will be a cause for disciplinary action by the Institute and can also evoke penal action from the sources that have thus not been properly cited, or from whom proper permission has not been taken when needed.

A rectangular box containing a handwritten signature in black ink. The signature appears to be 'N Bhugra'.

(Signature)

NIKHIL BHUGRA

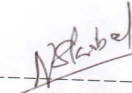
(– Student Name –)

EE11M08

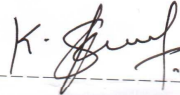
(Roll No)

## Approval Sheet

This thesis entitled Control Strategies for Wind-Solar Hybrid Energy Conversion System by Mr. Nikhil Bhugra is approved for the degree of Master of Technology from IIT Hyderabad.



-----  
Dr. Nandkishor Kubal  
Global Product Manager, ABB  
Examiner



-----  
Dr. Siva Kumar K.  
Assistant Professor, IIT Hyderabad  
Examiner



-----  
Dr. Ketan Detroja  
Assistant Professor, IIT Hyderabad  
Adviser



-----  
Dr. Ranjith Ramadurai  
Assistant Professor, IIT Hyderabad  
Chairman

# Abstract

Presently a lot of work is being carried in the field of distributed renewable generation. Many distributed generation systems are being designed and connected to the electric grid. At the time when the conventional sources of energy such as coal, oil, gas etc. are fast disappearing, a study of distributed renewable generation systems becomes very important.

When a DG source is being connected to the grid, there are many constraints to be met. This thesis mainly deals with the study, design, analysis and simulation of a wind-solar hybrid energy conversion system with grid-connection. This means that a proper control technique should be present in the system in order to coordinate the generation from the two renewable energy sources, such that all the grid constraints are met.

In this work, model predictive control technique is used as the master controller and limited power point tracking technique based controllers as the local controllers. Depending upon the load demand and other operating conditions, power reference from the master controller is given as input to the local controller. The limited power point tracking algorithm help us to remove expensive batteries from the circuit topology of the grid connected system. The validity of the control technique is verified through simulation under different operating conditions.

Overall, the project work involves study, design, modelling and simulation of wind-solar hybrid energy conversion system with grid-interface.

# Nomenclature:

SPVECS	: Solar photovoltaic energy conversion system
WECS	: Wind energy conversion system
MPPT	: Maximum power point tracking
MPP	: Maximum power point
LPPT	: Limited power point tracking
LPP	: Limited power point
HECS	: Hybrid energy conversion system
AC	: Alternating current
DC	: Direct current
MPC	: Model Predictive Control
VSI	: Voltage source inverter
CSI	: Current source inverter
PV	: Photovoltaic
WEC	: Wind energy conversion
PCC	: Point of common coupling
PSF	: Power signal feedback

## Table of Contents

<b>1 Introduction.....</b>	<b>1</b>
1.1 WEC and SPVEC modern systems: An Overview.....	3
1.2 Motivation.....	5
1.3 Scope of Work.....	6
1.4 Outline of chapters.....	6
<b>2 Literature Review .....</b>	<b>8</b>
2.1 Brief review on solar power conversion.....	8
2.2 Brief review on wind power conversion.....	11
2.2.1 Fixed speed wind turbines.....	13
2.2.2 Variable-speed /doubly-fed induction generator wind turbine .....	14
2.2.3 Full converter wind turbine.....	14
2.3 Brief review on different configurations of hybrid energy storage systems .....	16
2.3.1 WECS and SPVECS coupled at common DC bus .....	17
2.3.2 WECS and SPVECS coupled at common DC bus .....	18
2.4 MPPT control algorithms for SPVECS.....	19
2.5 MPPT control techniques for WECS .....	20
2.6 Brief review on control strategies for DC/DC converters .....	22
2.7 Brief review on control strategies for grid side VSI or CSI.....	22
2.8 Brief review on control strategies for SPVECS and WECS .....	23
2.8.1 Linear control techniques.....	23
2.8.2 Non linear control techniques .....	25
2.9 Introduction to advanced control techniques.....	26
2.9.1 Sliding mode control technique.....	26
2.9.2 Model predictive control .....	27
2.10 Conclusion.....	28
<b>3 Limited power point tracking for grid-connected SPVECS.....</b>	<b>29</b>
3.1 Solar power configuration.....	29
3.1.1 System description .....	29
3.1.2 System modeling .....	31
3.1.3 Control structure.....	32
3.2 Simulation and Results.....	36
3.3 Conclusion .....	40

<b>4 Limited power point tracking for grid-connected WECS.....</b>	<b>41</b>
4.1 Wind power configuration .....	41
4.1.1 System description .....	41
4.1.2 System modeling .....	43
4.1.3 Control structure.....	45
4.2 Simulation and Results .....	50
4.3 Conclusion .....	53
<b>5 Model Predictive Control implementation for grid-connected HECS.....</b>	<b>54</b>
5.1 Model predictive control.....	54
5.1.1 Prediction Model .....	55
5.1.2 Objective Function .....	56
5.1.3 Obtaining the control law .....	57
5.1.4 Model predictive control algorithms .....	57
5.2 Model predictive control implementation for SPVECS.....	57
5.2.1 Control architecture for SPVECS .....	57
5.2.2 Linearized state space model for SPVECS .....	58
5.2.3 Simulation and Results.....	59
5.3 Model predictive control implementation for WECS.....	60
5.3.1 Control architecture for WECS.....	60
5.3.2 Linearized state space model for WECS.....	61
5.3.3 Simulation and Results.....	62
5.4 MPC implementation of grid-connected HECS.....	63
5.4.1 Simulation and Results.....	63
5.5 Conclusion .....	65
<b>6 Conclusion.....</b>	<b>66</b>
<b>References.....</b>	<b>68</b>

## List of Figures:

	<b>Page no.</b>
Figure 2.1: Classification of the solar power converters depending on the stage of conversion	9
Figure 2.2: Single-phase two-stage grid-interfaced solar PV energy conversion system.	10
Figure 2.3: Single-stage single-phase grid interfaced solar PV energy conversion system.	10
Figure 2.4: Stand-alone isolated dc/dc converter (Cuk-converter) with single-phase inverter	10
Figure 2.5: Grid-connected isolated solar PV energy conversion system.	10
Figure 2.6: Type 1- Fixed Speed Wind Turbines	13
Figure 2.7: Type2/3 Variable Slip/ Doubly Fed Induction generator wind turbines	15
Figure 2.8: Uncontrolled rectifier and single phase inverter configuration	16
Figure 2.9: Controlled rectifier and single phase inverter configuration	16
Figure 2.10: Uncontrolled Rectifier and single phase inverter configuration with Intermediate converter	16
Figure 2.11: WECS and SPVECS coupled at common DC bus	17
Figure 2.12: WECS and SPVECS coupled at common AC Bus	18
Figure 2.14: Characteristic curve of PV	20
Figure 2.15: Wind turbine characteristics	21
Figure 2.16: Control architecture of SRS controller	24
Figure 2.17: Control architecture for LQR based SRS controller	25
Figure 2.18: Control architecture of fuzzy logic based controller	26
Figure 2.19: Sliding Mode Control State trajectories	26
Figure 2.20: Block Diagram of Model Predictive control	28
Figure 3.1: SPV system Configuration	31
Figure 3.2: Overall control system structure	32
Figure 3.3: Proposed Sliding mode control structure	35



Figure 3.4: Operating under step change in load demand	37
Figure 3.5: Response during Power insufficient mode	38
Figure 3.6: Response to sudden change in climatic condition	39
Figure 3.7: Response to load demand change during Islanded Mode	40
Figure 4.1: WECS system configuration	42
Figure 4.2: $C_p$ (Power Coefficient) Vs $\lambda$ (Speed tip Ratio)	44
Figure 4.3: Overall control system structure	47
Figure 4.4: Proposed LPPT controller (WECS)	48
Figure 4.5: Response to a step change in load demand	51
Figure 4.6: Operation under insufficient power condition	52
Figure 4.7: Operation under sudden climate change condition	53
Figure 5.1: Control architecture for solar energy conversion system	58
Figure 5.2: PV characteristic of solar module	58
Figure 5.3: Model predictive control implementation of solar energy conversion system	60
Figure 5.4: Control architecture for wind energy conversion system	61
Figure 5.5: Model predictive control implementation of wind energy conversion system	62
Figure 5.6: Control architecture for HECS	63
Figure 5.7: Model predictive control implementation of HECS	64

### List of Tables:

	<b>Page no.</b>
Table 3.1: SPVEC system parameters	30
Table 3.2: The PV panel parameters	30
Table 3.3: DC link voltage and hysteresis controller parameters (SPVECS)	36
Table 4.1: WEC system parameters	43
Table 4.2: Wind turbine parameters	43

Table 4.3: LPPT controller parameters	48
Table 4.4: DC link voltage and hysteresis controller parameters (WECS)	50

# Chapter 1

## Introduction

Major portion of the electric power in the world is produced using conventional sources of energy like coal, petroleum, natural gas etc., which are non-renewable. These conventional energy resources are available in limited quantities and are depleting very quickly. At the same time, demand for electric power is increasing day by day due to rising population, improved standard of living and economic development. Since these conventional resources are present in limited quantities the rising energy demand is forcing the prices of conventional sources of energy to increase. Further, the use of conventional sources of energy especially the fossil fuels have detrimental effect over the environment. Therefore, there is growing focus towards the use of renewable sources of energy like wind, solar, tidal, bio-fuels, fuel cell etc. Harnessing power from renewable sources of energy like solar or wind is one of the cleanest and most sustainable ways to generate electricity as they do not cause toxic pollution and global warming. Wind and solar energy sources are abundant, inexhaustible and affordable, which makes them viable. As these energy sources are capable of generating power at large-scale, they can be an alternatives to conventional sources of energy if energy can be harvested and transformed into electrical energy in a controlled fashion.

The energy generated from solar, wind or a hybrid system is generally in a form which cannot be used directly due to fluctuating voltage levels and/or frequency. Therefore it is necessary to process and transform the generated energy into suitable AC or DC form, depending on the requirement of the consumer load. The processing is done using controlled power electronic converters like DC/DC converters, rectifiers, inverters etc. Control techniques used for these converters play a crucial role in generating suitable AC or DC form. Various control techniques like hysteresis control,

PI control, synchronous reference frame control, fuzzy logic control etc. have been implemented for these power electronic converters. Recent advancements in power electronic devices and their control techniques have made the energy production by wind and solar more accessible and cheaper. Systems generating suitable AC or DC form from wind and solar energies are called wind energy conversion system (WECS) and solar photovoltaic energy conversion system (SPVECS) respectively.

Wind energy conversion systems (WECS) ranging from few kilowatts to gigawatts and solar photovoltaic energy conversion systems (SPVEC) ranging from few kilowatts to megawatts have been developed and installed. These renewable energy systems can be:

- Standalone/Isolated
- Grid connected

Standalone Systems are used for remote locations where grid connection is either not present or is not viable. These systems are not reliable because their output depends on the environmental conditions (e.g. solar radiation or wind speed). Energy storage devices like batteries are also necessary with the standalone systems to have reliable operation. Grid-connected WECS and SPVEC systems are more reliable than standalone systems as power can be extracted or dumped into the grid depending on load demand. Grid-connected WECS and SPVECS systems, when used independently, will have relatively more variation in the power input to the grid due to the environmental conditions. This may cause swings or transients in the power system if a large portion of power is being generated through these renewable energy sources. Integration of WECS and SPVECS into a single system, called a hybrid system, can reduce these fluctuations because of their complementary nature (in terms of availability).

Generally hybrid systems use maximum power point (MPP) control techniques for extraction of maximum power from both, solar and wind systems, irrespective of the load demand. So, high capacity energy storage systems are required to maintain power balance in the system. To minimize the need of high capacity batteries/dumping loads, limited power point (LPP) control techniques should be implemented and the hybrid system should be connected to the grid. Limited power point control techniques generate power based on load demand (or a reference value), i.e. when solar and/or wind energy is sufficient to satisfy the load requirements the system operates at a limited power point, and the system operates at maximum power points (MPP) under

insufficient energy conditions. Thus in both the cases excessive power, which was required to be dumped into batteries or dummy loads earlier, is never generated. Further, LPP control techniques reduce the dependence of hybrid system on grid.

Due to advancements in control techniques and efforts to make the system smarter, hybrid systems can be operated such that system reliability and efficiency increases and the system becomes more economical. Advanced control algorithms such as model predictive control (MPC), linear quadratic control (LQG) should be implemented to operate the system at optimum point while satisfying constraints on the system [1,2]. Typically a two stage hierarchal control architecture techniques are implemented for hybrid systems. First stage is a local controller (LPP) and the second stage is a supervisory controller based on MPC or LQR. Supervisory controller (MPC) calculates the optimized reference power point for the local controller based on future load predictions, environmental conditions and various constraints. Integration of MPC with LPP makes system more flexible.

### **1.1 WEC and SPVEC modern systems: An Overview**

A solar photovoltaic system uses solar cells to convert solar energy into electricity based on photovoltaic effect. Solar cell with maximum rating of 45 milliwatts is used in series and parallel combination to form a PV module of desired ratings. These PV modules are then used to form solar power plants. Solar power plants with ratings of 100-350 MW have been installed and are working efficiently across the world. With the advancement in semiconductor technology solar power plants with medium capacity ratings i.e. 500kw-10MW are being used at medium transmission level also.

These solar power plants are operated with maximum power point control techniques in order to make full utilization of the available solar power. Many algorithms for MPP control techniques have been developed such as perturb and observe (P&O), incremental conductance (IncCond), constant voltage operation etc[3]. A typical grid connected solar PV power conditioning system has two stages. The first stage is a DC-DC boost converter that boosts the PV array voltage and tracks the maximum power point of the connected solar PV array. Second stage is a inverter (VSI or CSI) that converts this dc power to ac power. Such two stage schemes are well known and have been implemented with various control algorithms.

Limited power point tracking technique controls the power coming from the SPV panels by controlling the switching signals of DC-DC (boost/buck) converters. Modified IncCond based algorithm controller, sliding mode controller etc techniques have been implemented for standalone, battery connected systems[4]. However these LPP control techniques are very few compared to MPP control algorithms.

A WECS converts mechanical energy into electrical energy with the help of turbines and generators. A wind turbine is a device that converts the kinetic energy from the wind into mechanical energy. These wind turbines are coupled to synchronous or asynchronous generators (depending on the rating of the wind power plants) through a drive train. Wind power plants with ratings from few kilowatts to gigawatts have been installed across the world. Medium scale power plants with capacities of 100 MW are also being used at medium transmission level.

A typical grid connected wind energy power conditioning unit has broadly two stages. The first stage is preferably a converter (Controlled or Uncontrolled) that converts the three phase voltage of generator to dc. The second stage converts this dc power to ac power through VSI or CSI. There can be an intermediate stage also which can be a DC-DC boost converter to boost the inverter end's dc voltage. The WEC systems are operated with maximum power point tracking algorithms. The maximum power point tracking for wind energy conversions system is done through the pitch/stall angle control of the wind turbine because power output depends on the wind speed and rotor speed [5].

Limited power point tracking technique controls the power coming from the WECS by controlling the switching signals of DC-DC (boost/buck) converters. Modified IncCond based algorithm controller, sliding mode controller etc techniques have been implemented for standalone battery connected systems. As in the case of SPECS systems, very few LPP control techniques have been proposed for WECS compared to MPP control algorithms.

As mentioned earlier, installation of high capacity solar power plants has encouraged the integration of solar and wind systems at high and medium transmission level. . Hybrid system with the ratings 30-70kw has been installed in India. Due to complementary nature of the SPV and wind systems, hybrid system turns out to be a more reliable system in terms of availability of power from the system. Hybrid system also makes the system economical because wind turbines are less expensive than solar panels of same capacity, so places where average solar irradiation is above 0.5pu and

average wind speed is above 5m/sec, combining solar and wind systems can result in a good tradeoff between investment cost and power output. An additional benefit with the construction of hybrid system is that they don't require grid expansion because of their complementary nature.

Hybrid systems can be broadly divided into two types: standalone and grid connected systems [6,7]. There can be two ways in which the PV-wind systems can be coupled with each other (i) coupled at the common dc link bus (ii) coupled at the point of common coupling [8,9]. With the advancement in the semiconductor technology, several classifications of converter topologies can be done with respect to the number of processing stages, use of transformers and types of grid interface.

## **1.2 Motivation**

As discussed above (section 1.1), most efforts (if any) have been made to implement LPP control techniques for standalone, battery connected systems. While in standalone systems batteries may be unavoidable due to stability and reliability aspects of the system, in grid-connected systems these batteries are not essential. However most of the systems have a battery backup. Some of the main reasons why batteries should be minimized or eliminated are: i) initial investment of batteries is very high and including batteries would result in higher capital cost of renewable energy system. ii) Maintenance cost of the batteries is also high as life of batteries is much less compared to other renewable energy system components. And iii) used batteries have a significant impact on environment and cost of safely discarding these batteries is considerable. In spite of these disadvantages, due to lack of proper control strategies, batteries are invariably connected at DC link of SPVECS and WECS in order to keep DC link voltage constant. Thus there is a need to develop control strategies for grid-connected, battery free hybrid systems.

During this thesis research, the main focus was on proposing control architecture for grid-connected hybrid system that can operate SPVECS and WECS at limited power points and at the same time maintain DC link voltage constant without the use of batteries. Elimination of batteries from such systems will reduce the cost of whole system and also eliminate issues related to batteries like constant maintenance, control of battery charging and discharging, over voltages etc. Further, optimizing the system performance, in presence of various environmental and system constraints,

was also another aspect considered in this research work. Scope of the work is outlined in the next section.

### **1.3 Scope of work**

Research on LPPT (Limited Power Point Tracking) based control algorithms for hybrid systems in comparison to the MPPT (Maximum Power Point Tracking) based control algorithm is less. However, due to high battery prices and need for a cheap renewable sustainable hybrid energy source, LPPT based algorithms offers a viable alternative. It is important to decrease the overall cost and at the same time improve reliability of these systems. Intelligent control schemes are needed to meet the stringent standards and for efficient utilization of various components [10]. With respect to these issues main objectives of this research are

- Analysis, design, control and simulation of grid-connected, three-phase, two-stage hybrid systems with LPPT controller.
- Analysis, design, control and simulation of grid-connected, three-phase, two-stage hybrid system with supervisory controller for overall cost minimization.
- Highlighting the advantages of using hybrid system with the proposed LPPT control techniques over the MPPT control techniques by eliminating the requirement of energy storage system
- Highlighting the advantages of using an optimal control strategy for hybrid system.

### **1.4 Outline of chapters**

This chapter gives an introduction and general features of solar and wind energy, hybrid systems. It also specifies the objectives of this project work in precise and orientation of the thesis.

**Chapter 2:** This chapter covers the literature survey on hybrid systems, MPPT techniques, hybrid Systems configurations, control techniques.

**Chapter 3:** This Chapter deals with the implementation of limited power point tracking controller for grid connected solar PV energy conversion systems.

**Chapter 4:** This Chapter deals with the implementation of limited power point tracking controller for grid connected wind energy conversion systems.



**Chapter 5:** This chapter deals with the integration and implementation of PV-Wind grid connected systems with Model Predictive Controller and Limited Power point Tracking Controller.

**Chapter 6:** This Chapter deals with the final conclusions on the basis of this study. Suggestions for future work are also given at the end of the thesis.

# Chapter 2

## Literature Review

A brief introduction, highlighting main focus of the thesis was given in the previous chapter. This chapter consists of a brief literature survey, which covers various configurations of the solar power converters, wind energy conversion systems (WECS) and hybrid renewable energy systems (HERS), maximum power point tracking (MPPT) techniques, sliding mode controller and model Predictive controller (MPC).

### 2.1 Brief review on solar power conversion

A solar photovoltaic system uses solar cells to convert solar energy into electricity based on photovoltaic (PV) effect. The PV systems directly convert solar energy into electricity.

SPVEC systems are broadly divided into two types: standalone and grid-connected [11,12,13,14]. Several classifications of SPVECS can also be done with respect to the number of processing stages, location of power-decoupling capacitors, use of transformers and types of grid interface as shown in Figure 2.1.

As discussed in chapter 1, grid-connected SPVEC systems are more reliable than standalone SPVEC systems. Therefore main literature survey is focused on grid-connected SPVEC systems. A typical two-stage (Figure 2.2) grid-connected solar PV power conditioning unit has two stages. The first stage is preferably a DC-DC converter that boosts the PV array voltage and tracks the maximum power point of the connected solar PV array. The second stage converts this dc power to ac power. Such two stage schemes are well known and implemented in wide rating of solar PV system. These two stage configurations have low efficiency, high component count and low reliability. In spite of the disadvantages a two-stage configuration has, this type of topology is a necessity for large solar plants where distributed MPPT is required in order to offset the effects of PV array mismatch, partial shading and where MPPT

cannot be performed by a single central inverter. The main advantage of the two stage topology is the flexibility of designing its control scheme since it has higher freedom degree, i.e. more controllable variables, which means multiple control objectives (MPPT, grid connecting, var compensating, active filter, etc) can be shared by two stages simultaneously.

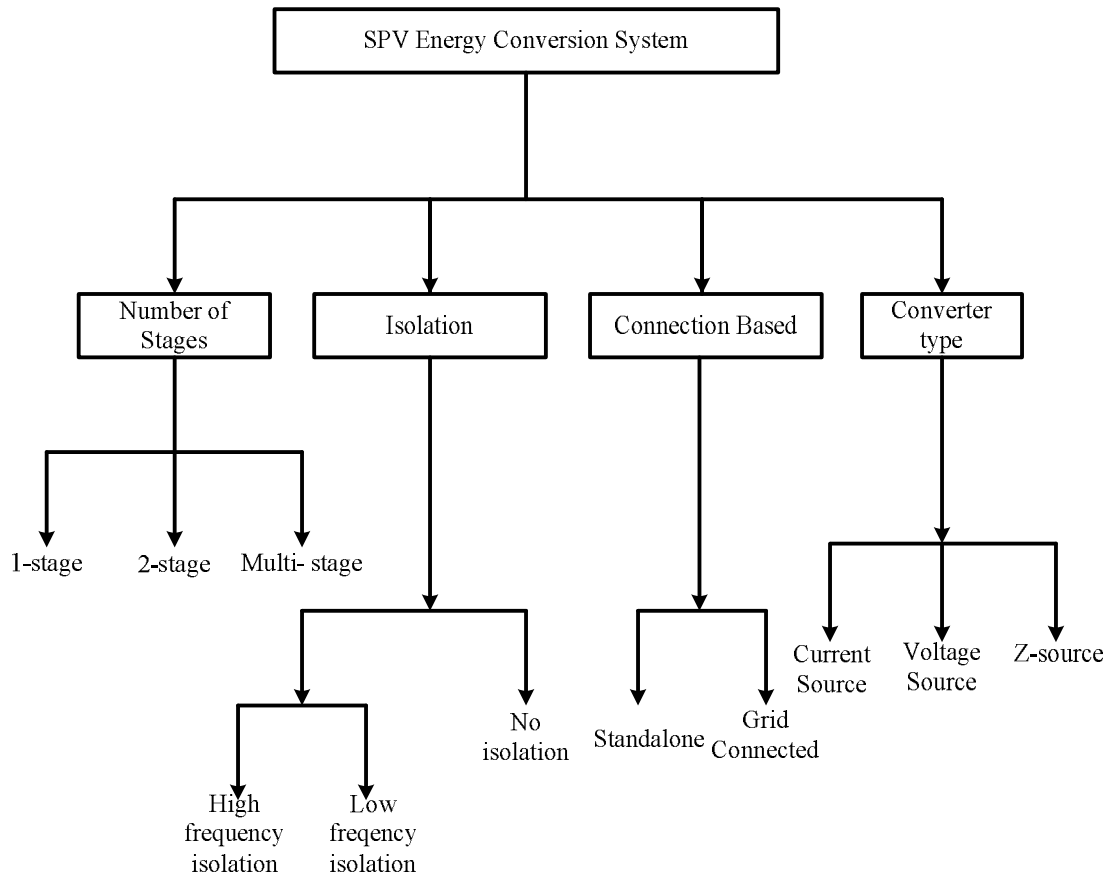


**Figure 2.1: Classification of the solar power converters depending on the stage of conversion**

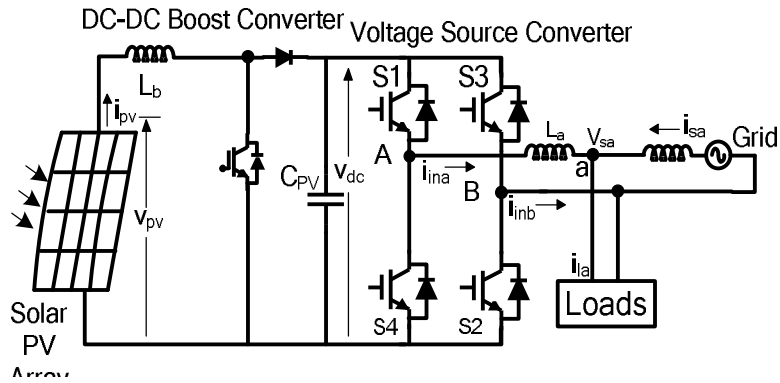


Figure 2.2: Single-phase two-stage grid-interfaced solar PV energy conversion system.

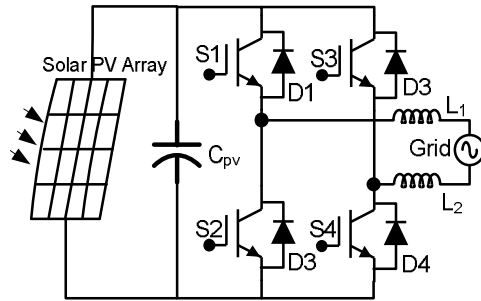


Figure 2.3: Single-stage single-phase grid interfaced solar PV energy conversion system.

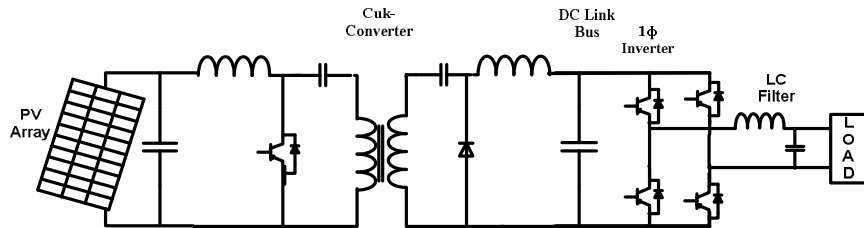


Figure 2.4: Stand-alone isolated dc/dc converter (Cuk-converter) with single-phase inverter

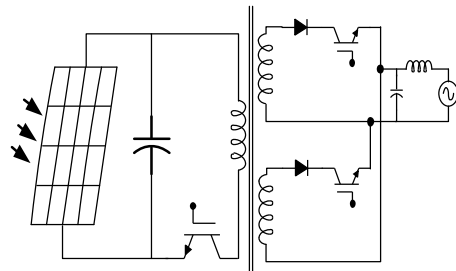


Figure 2.5: Grid-connected isolated solar PV energy conversion system.

A typical single-stage (Figure 2.3) grid interfaced solar PV energy conversion systems consist of only voltage source inverter (commonly used) or current source inverter (rarely used) which converts DC from solar cells to suitable AC form. Since VSI's have voltage down property the use of 1-stage grid interfaced SPVEC configuration is limited to small and medium power ratings. Single-stage systems have higher efficiency as compared to two-stage systems but its MPPT performance is poor as compared to two stage-systems[15,16,17].

On the basis of connection of DC/DC converters with the VSI's or CSI's the SPVECS system can be classified in two ways i) isolated ii) non isolated. Isolated converters (Figure 2.5) are used at places where the difference in voltages of the PV array and the battery is high. DC/DC converter must utilize isolation transformer for compensating duty cycle and safety problems. There are various isolated DC/DC converters like bi-directional cuk converter (Figure 2.4), bi-directional full bridge converter, bi directional half bridge converter etc. Non isolated converters are generally used for small and medium power plants. Buck converter, Boost converter and Buck-Boost converters are the basic non isolated DC/DC converters

SPVECS can also be classified based on the converter type, primarily used for interfacing the solar photovoltaic system with the grid. It can be broadly divided into three types i) Voltage source inverters (VSI) ii) Current Source Inverter (CSI) iii) Z source inverter .VSI's are generally preferred over CSI's because VSI's have low switching losses and are cheaper. Z source inverter is new area of research, but it is proving out to be a better option than VSI's for single-stage grid connected SPVEC systems. Z source inverters are power electronic devices that perform boosting up operation and conversion of DC to AC power at the same time.

## **2.2 Brief review on wind power conversion**

A wind energy conversion system (WECS) converts the kinetic energy of wind speed into electrical energy with the help of wind turbines (wind mills coupled with generators). Wind mill convert the kinetic energy of the wind into mechanical energy. Windmills are coupled to synchronous/asynchronous generators through a drive train. The generators convert the mechanical energy of wind mill to electrical energy (AC form). Electrical energy obtained from the generators is converted into suitable AC or DC form depending on the requirement at consumer side.

A WEC system can be broadly classified in two ways i) standalone and ii) grid connected. As discussed in chapter 1, grid-connected WEC systems are more reliable than standalone WEC system. Therefore main literature survey is focused on grid-connected WECS.

A typical grid-connected WECS consists of two stages. First stage is the controlled/uncontrolled converter which operates the wind turbine at maximum power points (when using controlled converter) and converts the AC output of the generator into suitable DC form. Second stage is essentially a VSI or CSI which interfaces the wind system to grid. A DC/DC boost converter intermediate stage can also be there. DC/DC boost converter is connected between first and second stage. It is used to boost up the voltage for VSI's DC end voltage.

WECS can also be classified on the basis of wind turbines being used. A wide variety of wind turbines are in use today. Typical wind power plants consist of hundreds of turbines, usually all employing the same technology. These turbines vary in cost, complexity, efficiency of wind power extraction and equipments used [18]. A typical wind turbine employs a blade and hub rotor assembly to extract power from the wind, a gear train to step up the shaft speed at the slowly-spinning rotor to the higher speeds needed to drive the generator and an induction generator as an electromechanical energy conversion device. Induction machines are popular as generating units due to their asynchronous nature, since maintaining a constant synchronous speed in order to use a synchronous generator is difficult due to variable nature of wind speed. Power electronic converters may be used to regulate the real and reactive power out of the turbine. In [23], wind turbines have been classified into four basic types:

- Type 1: Fixed-speed Wind Turbines, Fig 2.6
- Type 2: Variable-Slip Wind Turbines, Fig 2.7
- Type 3: Doubly-Fed induction generator (DFIG) Wind Turbines, Fig 2.7
- Type 4: Full-converter wind turbines, Fig 2.8, 2.9, 2.10

Various wind energy conversion system using different wind turbines are –

### **2.2.1 Fixed speed wind turbines**

Fixed-speed turbines, as shown in Figure 2.6, are the most basic utility-scale wind turbines in operation. They operate with very little variation in turbine rotor speed, and employ squirrel-cage induction machines directly coupled to the grid.

Fixed speed wind turbines can be connected to grid in various configurations. These are based on number of stages of electric power conversions. These configurations are:

1. Direct Connected: Output of the squirrel-cage induction machine is directly connected to the grid
2. Back to back PWM: Output of the induction generator is connected to uncontrolled rectifier, which is connected to controlled inverter.
3. Back to back PWM with intermediated dc/dc converter: a dc/dc boost converter is connected between the uncontrolled rectifier and controlled inverter.

Advantages and disadvantages of fixed speed wind turbines:

Advantages:

- Relatively Robust
- Reliable

Disadvantages:

- Energy capture from the wind is sub optimal
- Reactive power compensation is required

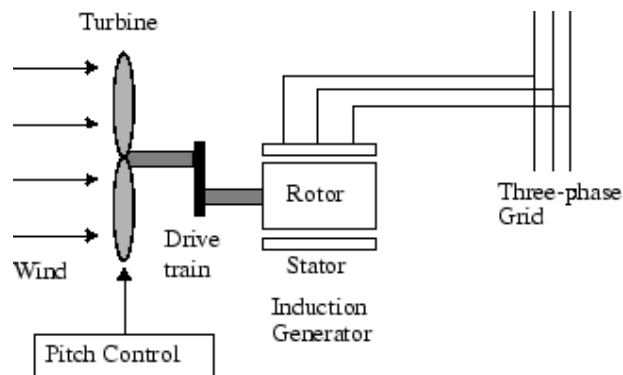


**Figure 2.6: Type 1- Fixed Speed Wind Turbines**

### **2.2.2 Variable-speed /doubly-fed induction generator wind turbine**

Variable-speed wind turbines, as shown in Figure 2.7, are designed to operate at a wide range of rotor speeds. These turbines usually employ blade pitching. Speed and power control allow these turbines to extract more energy from a given wind speed regime than fixed turbines can. In a singly fed induction machine the variable slip

operation is achieved by dynamically controlling the resistance in the rotor circuit of the machine. However power is lost as heat in the rotor resistance, So DFIG (doubly fed induction generator) turbines remedy to this problem by employing back to back AC/DC/AC converter in the rotor circuit to recover the slip power.

Variable speed wind turbines can be connected to grid in various configurations. These are based on number of stages of electric power conversions. These configurations are:

1. Back to back PWM (uncontrolled/controlled converter-to-controlled inverter)
2. Back to back PWM with intermediate DC/DC converter

Some advantages and disadvantages of variable speed wind turbines:

Advantages:

- Reduced converter cost
- Improved efficiency due to reduced losses in the power electronic converter
- Control may be applied to the lower cost due to reduced converter power rating

Disadvantages:

- Increased control complexity due to increased number of switches in converters
- Increased capital cost and need for periodic slip ring maintenance

### **2.2.3 Full converter wind turbine**

In full converter wind turbines, a back to back AC/DC/AC converter is the only power flow path from the wind turbine to the grid. There is no direct connection to the grid. These turbines employ synchronous generators and offer independent real and reactive power control. Full converter wind turbines can be connected to grid in various configurations. These are based on number of stages of electric power conversions. These configurations are:

1. Back to back PWM (Figure 2.8) (uncontrolled/controlled converter-to-controlled inverter)
2. Back to back PWM with intermediate DC/DC converter (Figure 2.9, 2.10)

Some advantages and disadvantages of full converter wind turbines:

Advantages:

- Flexibility in design allows for smaller and lighter designs



- Higher output level may be achieved. Fundamental Component is more in PMLDC while compared with the PMSM
- Lower maintenance cost and lower losses

Disadvantages:

- High Initial cost due to high price of magnets used.

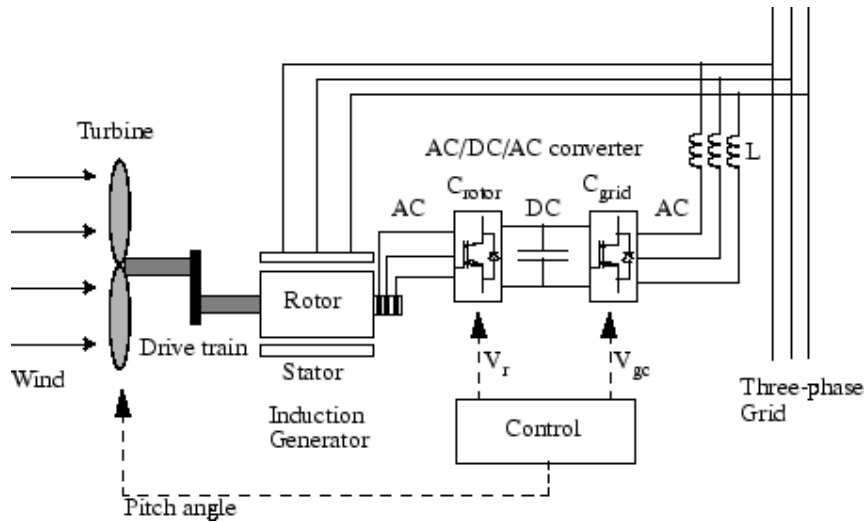


**Figure 2.7: Type2/3 Variable Slip/ Doubly Fed Induction generator wind turbines**

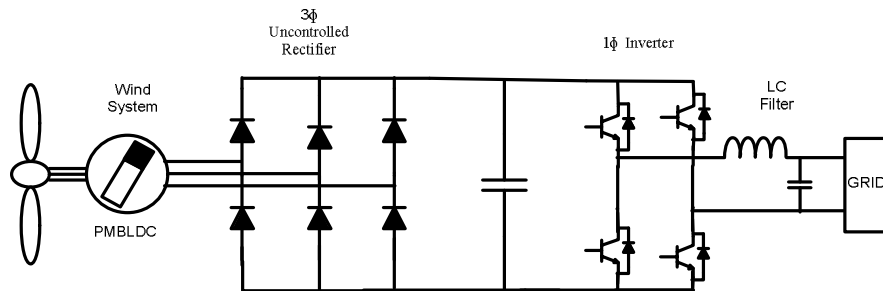


**Figure 2.8: Uncontrolled rectifier and single phase inverter configuration**

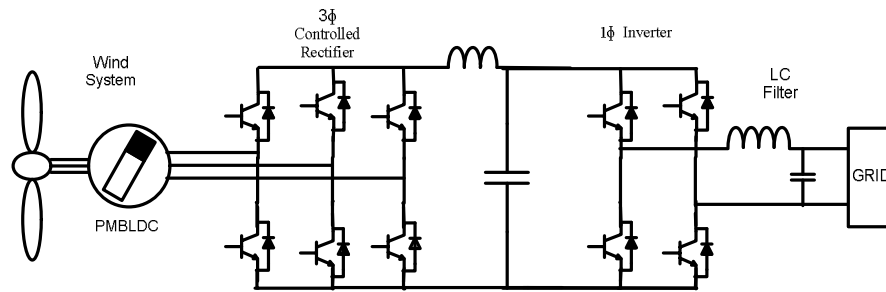


**Figure 2.9: Controlled rectifier and single phase inverter configuration**

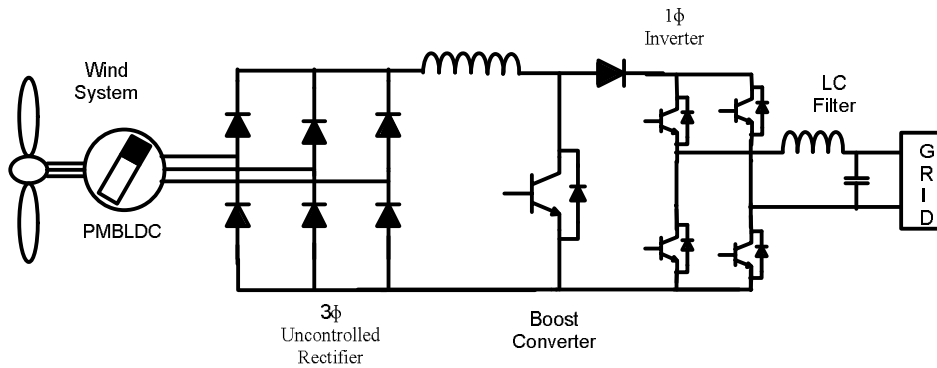


**Figure 2.10: Uncontrolled Rectifier and single phase inverter configuration with Intermediate converter**

### 2.3 Brief review on different configurations of hybrid energy storage systems

PV-Wind hybrid systems configurations can be broadly divided in two ways i) PV-Wind hybrid systems coupled at common DC bus and ii) at common AC bus. These configurations of Solar PV-Wind Hybrid Systems are discussed below [19, 20, 21].

#### 2.3.1 WECS and SPVECS coupled at common DC bus

Generally WECS and SPVEC systems are integrated at common DC bus, shown in Figure 2.11.

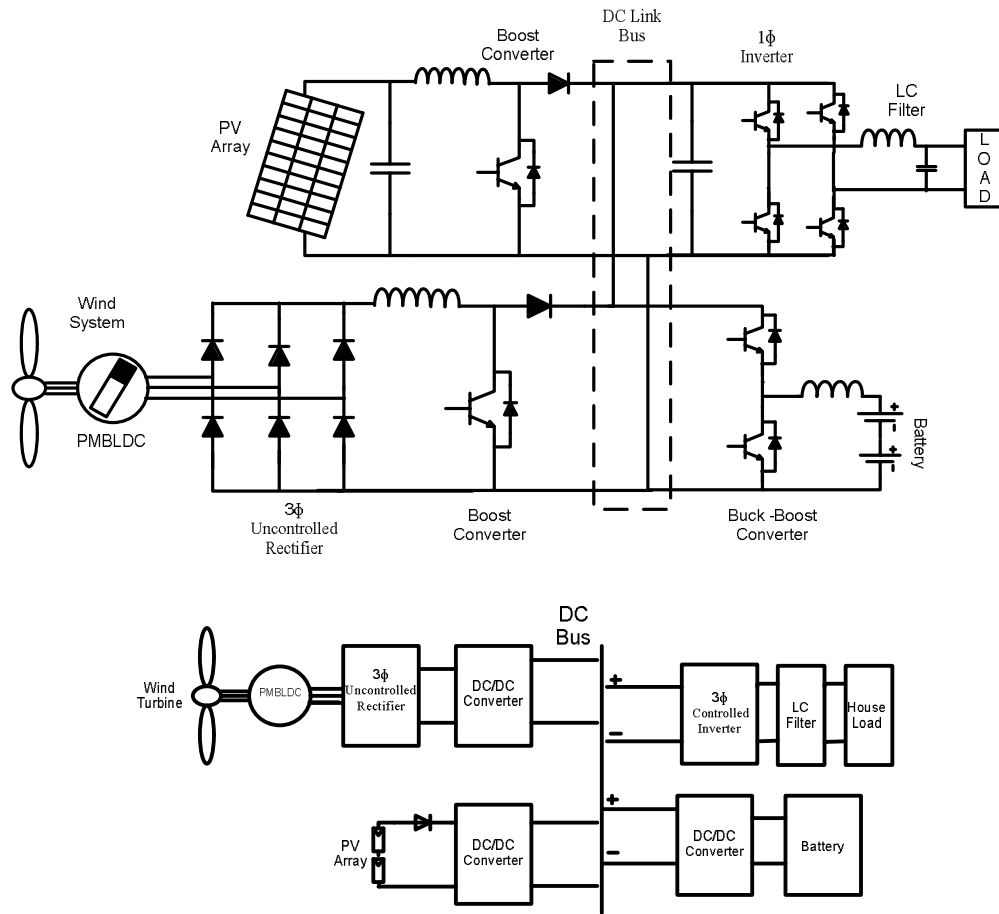


**Figure 2.11: WECS and SPVECS coupled at common DC bus**

Some advantages and disadvantages of integration of SPVECS and WECS at common DC bus.

Advantages:

- It is having the common dc bus voltage which is very flexible for interconnection of systems.
- Each stage can be easily controlled with simple control system
- Only one Inverter is present, which is used for supplying the ac load
- Reliability of the system is High

Disadvantages:

- It is a two-stage converter which results in more losses, hence low efficiency
- More number of switches is used, hence cost will be more.

### 2.3.2 WECS and SPVECS coupled at common AC bus

WECS and SPVEC systems can also be connected at point of common coupling (PCC), shown in Figure 2.12

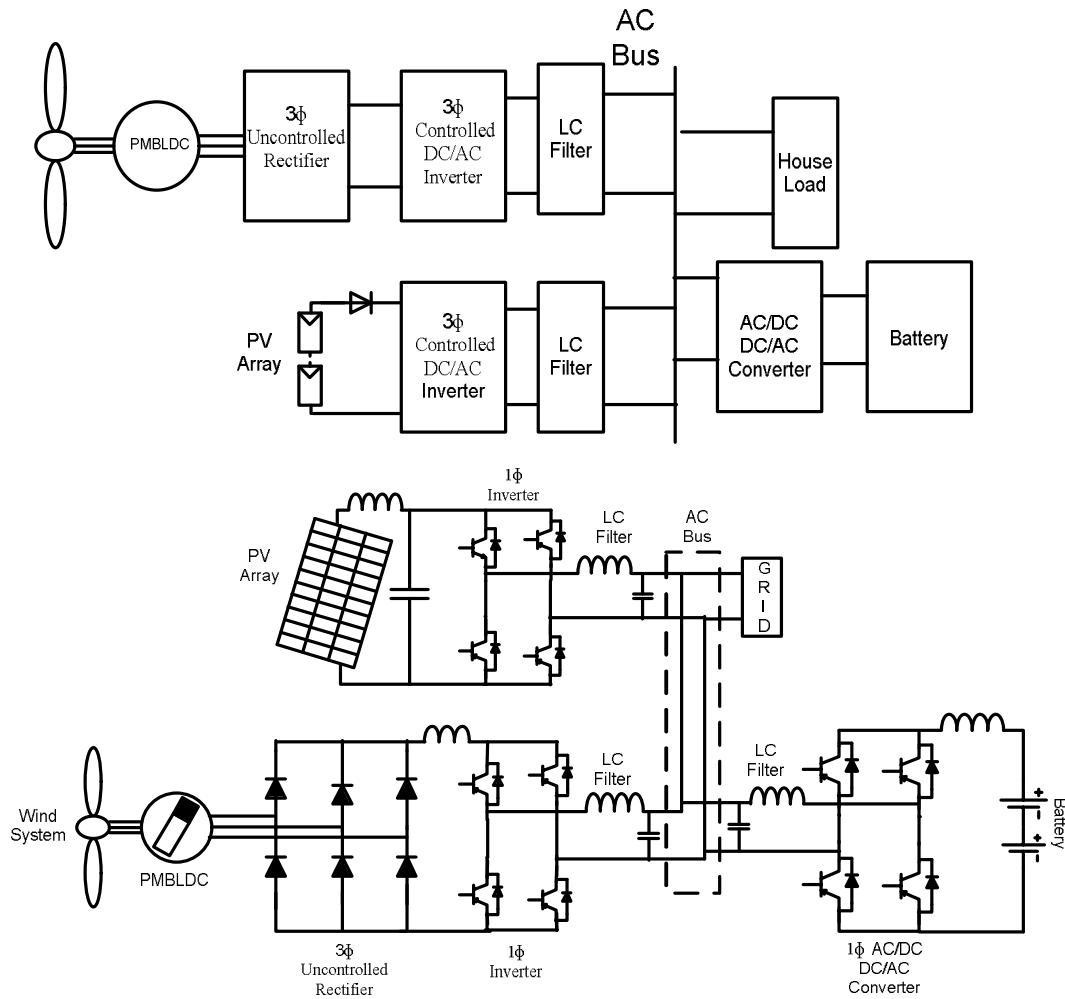


**Figure 2.12: WECS and SPVECS coupled at common AC Bus**

Some advantages and disadvantages of integration of SPVECS and WECS at common AC bus:

Advantages:

- Numbers of switches are reduced, cost is low, switching is low and efficiency is high.
- It occupies less space/volume for installation

Disadvantages:

- At the ac bus , synchronization problem will occur

- Control strategy will be more complicated

## 2.4 MPPT control algorithms for SPVECS

MPPT control algorithms are used to extract the maximum electrical power from the solar cells. These maximum power points are the system operating points at which we get the maximum power output from the system. Implementation of MPPT result in 40% more efficient systems than the systems operating without the maximum point algorithms.

- The most common MPPT algorithms are –
  - Hill Climbing method (P&O Algorithm)
  - Incremental Conductance method
  - Constant Voltage Method
  - Modified hill climbing method
  - $\beta$  method

**Hill climbing method (or P&O algorithm):** Hill climbing method is a modified form of perturb and observe MPPT algorithm. Among various MPPT algorithms main focus has been on hill climbing method [3] and P&O [3]. DC/DC converters are used to control the PV array output voltage. Hill climbing involves a perturbation in the duty ratio of the power converter and P&O a perturbation in the operating voltage of the PV array. Perturbing the duty ratio of a power converter perturbs PV array current and consequently perturbs the PV array voltage.

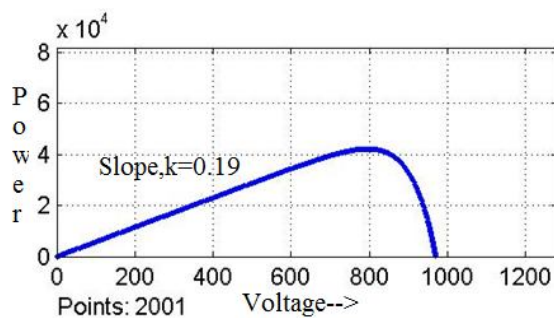


**Figure 2.14: Characteristic curve of PV**

As can be seen in Figure 2.14 that incrementing (decrementing) the voltage increases (decreases) the power when operating on the left of the MPP. Therefore, if there is an increase in power, the subsequent perturbation should be kept in the same direction in

order to reach the MPP and if there is a decrease in power, the perturbation direction should be reversed.

**Incremental conductance:** The incremental conductance (IncCond) [22,23] method is based on the fact that the slope of the PV array power curve (Figure 2.14) is zero at the MPP, positive on the left of the MPP, and negative on the right. MPP is tracked by comparing the instantaneous conductance ( $I/V$ ) to the incremental conductance ( $\Delta I/\Delta V$ ), where  $I$  is the PV array output current and  $V$  is the PV array output voltage. Based on the comparison IncCond decides the operating reference voltage for converter controller.

A lot of research has been done on MPPT control techniques for DC/DC converters [24,25,26] in SPVECS. But very less amount of work has been done on the limited power point tracking control technique for DC/DC converters in SPVECS.

## 2.5 MPPT control techniques for WECS

A lot of literature can be found on maximum power point control strategies for WECS [27,28]. The most commonly used MPPT control techniques are:

- Tip speed ratio control
- Power signal feedback control
- Hill climb search control
- Pitch control

**Tip speed ratio control (TSR):** A wind speed estimation based TSR control is proposed in [32] in order to track the peak power points. The wind speed is estimated using neural networks, and further, using the estimated wind speed and knowledge of optimal TSR, the optimal rotor speed command is computed. The generated optimal speed command is applied to speed control loop of the WECS control system. The PI controller controls the actual rotor speed to the desired value by varying the switching

ratio of the PWM inverter. The optimal speed is obtained using  $\lambda_{opt} = \frac{w_{ref} R}{v_{est}}$  where

$\lambda_{opt}$  is optimal tip speed ratio (TSR),  $R$  is the radius of turbine,  $v_{est}$  is estimated wind speed,  $w_{ref}$  the reference speed to be generated.

**Power signal feedback control:** In [32] turbine power equation(2.1) is used in for obtaining reference power for PSF based MPPT control. The reference power obtained

is given to PI controller which controls the actual power to the desired value by varying the switching ratio of PWM.

$$P_{opt} = K_{opt} w_r^3 \quad (2.1)$$

**Pitch/Stall control:** The pitch angle of the blade is controlled in order to keep WECS at rated power. The reference for pitch angle is determined by using wind turbine characteristics shown in Figure 2.15 where  $C_p$  is power coefficient and  $\lambda$  is turbine tip speed ratio. The reference pitch angle is then given to PI controller which varies the actuators. The reference pitch angle is obtained using empirical relation between

$$C_p, \lambda, \beta \text{ (pitch angle) given by } \beta_{ref} = \sqrt{\frac{1}{0.022} [\lambda - 5.6 - 2C_p e^{0.17\lambda}]}$$

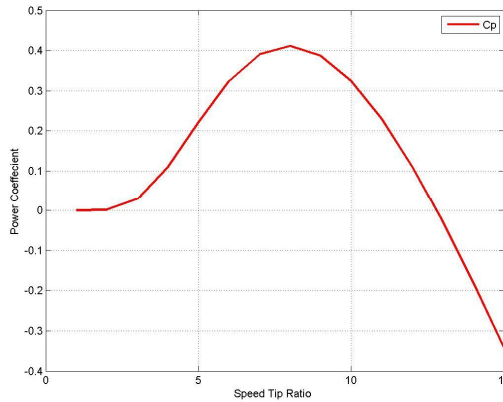


**Figure 2.15: Wind turbine characteristics**

A lot of research has been done on MPPT control techniques for maximum power point tracking. Very less amount of work has been done on limited power point tracking of WECS.

## 2.6 Brief review on control strategies for DC/DC converters

DC/DC converters are used in SPVECS system to extract maximum power from solar and boosting the inverter end's voltage. There are various control techniques to control the DC/DC converter (Buck or Boost). Control has two parts. First is MPP algorithm and second is tracking of reference point obtained from MPP. Main focus has been on MPP algorithms as discussed in section 2.6. Second part of control is generally a PI control. The voltage reference point obtained from MPPT algorithms is given to PI control. PI control minimizes the difference in actual voltage of PV array and the

reference voltage set by MPP algorithms. The output of PI is given as reference signals to the pulse width modulator.

DC/DC converters in WECS systems are generally used to boost up the voltage. PID controllers are the most commonly used technique for boosting the output voltage and maintaining it constant. The PID control minimizes the difference between actual output voltage and reference output voltage. The output of the PID control is used as reference signals for pulse width modulator to generate switching signals for DC/DC converter. The PID control can cope reasonably well with systems having different types of dynamic.

## **2.7 Brief review on control strategies for grid side VSI or CSI**

Generally voltage source inverter is preferred over current source inverter. Current source inverters have high switching losses and are more costly than voltage source inverters. Many control techniques of VSIs can be found. Most commonly used control techniques are:

- Stationary controller PI
- Synchronous vector controller PI
- State feedback controller
- Predictive and Deadbeat controller
- Proportional resonant controller
- Hysteresis controller

**Stationary controller PI:** It is also called ramp comparison controller, uses three PI error compensators to produce the voltage commands for a three phase sinusoidal PWM [29]. In keeping with the principle of sinusoidal PWM, comparison with the triangular carrier signal generates control signals for the inverter switches. Controller performance is satisfactory only if the significant harmonics of current commands and load EMF are limited at a frequency well below the carrier. The main disadvantage of this technique is inherent tracking (amplitude and phase) error

**Synchronous vector controller (PI):** The controller uses two PI compensators of current vector components defined in rotating synchronous coordinate's d-q [30]. The current vector reference in d-q frame from the supervisory control is given to these PI controllers which controls the amount of power to be transferred by varying the switching ratio of the inverter's switches.



**Hysteresis controller:** Hysteresis control schemes are based on nonlinear feedback loop with two-level hysteresis comparators. The switching signals are produced directly when the difference between the reference current and the instantaneous currents exceeds an assigned tolerance band [31,32].

## 2.8 Brief review on control strategies for SPVECS and WECS

In this some control strategies for SPVECS and WECS have been discussed

**2.8.1 Linear control techniques:** SPVECS interfaced to grid with synchronous reference frame theory based control technique has been implemented in [33]. Control is based on an inner current control loop and outer dc link voltage regulator. The dc-link voltage-control scheme enables control and maximization of power output. The dc-link voltage control implements a PI control cascaded with a low pass filters which gives current reference to the SRS based inner current control loop. In inner current control loop the three phase current is converted into synchronous reference frame (dq) .Two PI controllers cascaded with a decouple controller along with feed forward compensation for tracking of  $i_d, i_q$  is implemented. The output of these controllers decides the switching signals for interfacing VSI. Control architecture of this system is shown in Figure 2.16

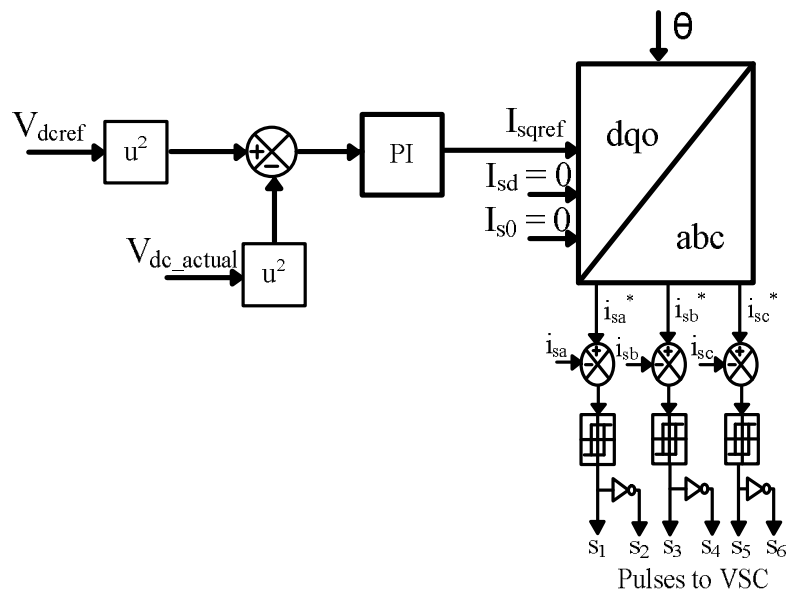


**Figure 2.16: Control architecture of SRS controller**

Advantages

- DC link voltage maintained constant without batteries
- No extra control technique is required for grid synchronization

Disadvantages

- For standalone systems the control technique will not work as it always operated at maximum power point

WECS interfaced to grid with linear quadratic regulator (LQR) based techniques has been implemented in [34]. Due to multivariable nature of the WECS, LQR based control technique has been implemented. State space model of the whole system is obtained in synchronous reference frame (dq). Using dq frame state space model and a user defined cost function, the LQR algorithm returns a constant control matrix  $K$  that minimizes the cost function by using  $u = -Kx$  control law where  $u$  is the control input and  $x$  is the states  $(i_d, i_q)$ . LQR controller decides the switching signal for VSI.

Control architecture of this system is shown in Figure 2.17

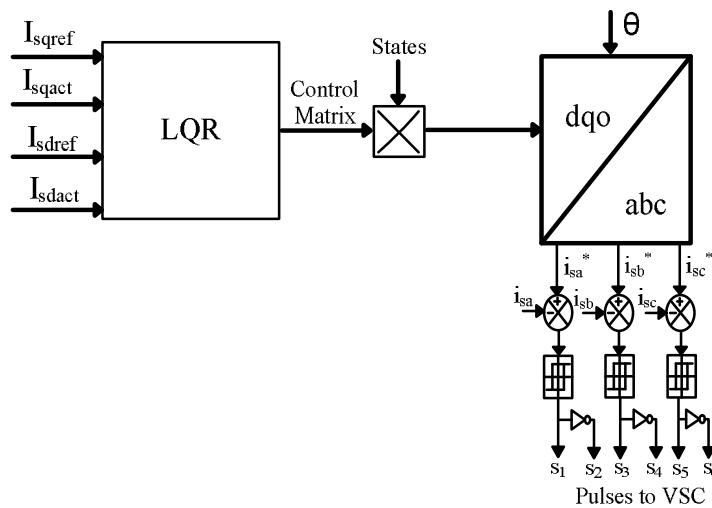


**Figure 2.17: Control architecture for LQR based SRS controller**

Advantages

- Elimination of harmonics can be done based on cost function
- Additional control technique for grid synchronization is not required

Disadvantages

- Tuning parameters  $Q, R$  have to be tuned accurately.
- Tuning parameters change with change in user defined cost function

**2.8.2 Nonlinear control technique:** WECS interfaced to grid with fuzzy based control technique has been implemented in [35]. With a predefined wind turbine characteristic and membership functions developed based on experience, fuzzy logic controller is operated under limited power point or maximum power point. The output for the fuzzy logic controller is the desired reference speed of the generator. Variable speed control technique of PMSG is then used to track the reference speed. Control architecture of this system is shown in Figure 2.18

Advantages

- LPP operation can be performed

Disadvantages

- Difficult to design membership function as it is based on experience

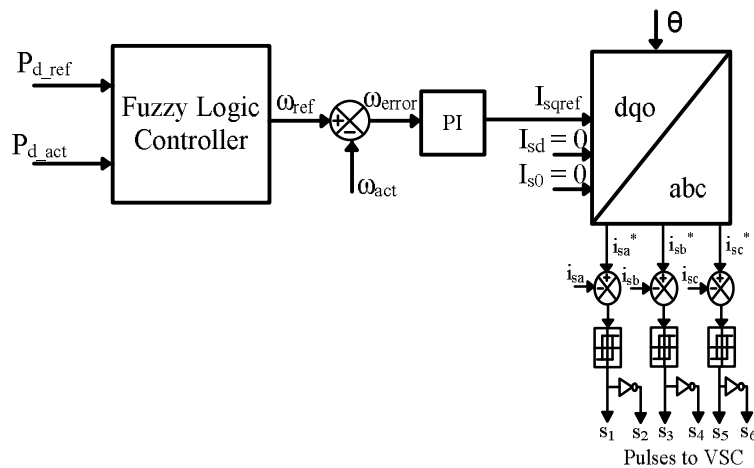


Figure 2.18: Control architecture of fuzzy logic based controller

## 2.9 Introduction to advanced control techniques:

### 2.9.1 Sliding mode control technique:

Sliding mode control [36] is a nonlinear control method that alters the dynamics of a non-linear system by application of a discontinuous control signal that forces the system to slide along a cross section of the system's normal behavior. The state feedback control law is not a continuous function of time. Instead it can switch from one continuous control structure to another based on the current position in the state

space. Sliding mode control is a variable structure control technique. To accomplish desired state trajectories an ‘overshoot and instantaneous correction’ approach is employed by switching between two possible feedback loops. In Fig 2.19 it is shown that a surface  $S=0$  is defined that constraints the states of the system  $X_1$  and  $X_2$  along the desired trajectories.  $S=0$  defines the control law for the system.

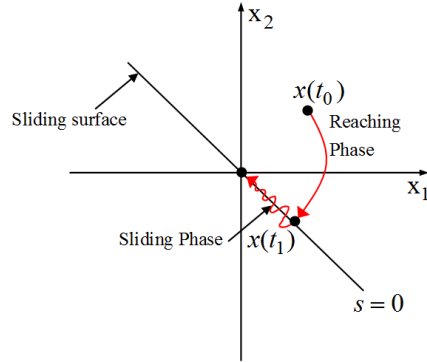


**Figure 2.19: Sliding Mode Control State trajectories**

**2.9.2 Model predictive control technique:**

Model Predictive control [37] is a class of control strategies based on the explicit use of a process model to generate the predicted values of the output at future time instants, which are then used to compute a sequence of control moves that optimize the future behavior of a plant. The set of future control signals is calculated by optimizing a given criterion called objective function or performance index in order to keep the system as close as possible to reference trajectories. Objective function shown in Equation (1.1) is generally in the form of quadratic function of the errors between the predicted output signal and the predicted reference trajectories. The control effort is included in the objective function in most cases. Weights are used to adjust the influence of each term in the equation. The solution of the problem is the future control sequence that minimizes the objective function.

A typical objective function is:

$$J(N1, N2, N3) = \sum_{j=N1}^{N2} \hat{y}(t+j|t) - w(t+j) \square^2 R + \sum_{j=1}^{N3} \square \Delta u(t+j|t) \square^2 Q \quad (2.2)$$

It is a quadratic function with  $u(t+j)$  the future inputs, and the error between the future values of reference output  $w(t+j)$  and predicted outputs

$\hat{y}(t+j|t)$ . Weights  $R$  and  $Q$  are used to adjust the error and the inputs respectively.  $N2 - N1$  is the prediction horizon,  $N3$  is the control horizon.

Model Predictive Control (MPC) technique is used in this research work, which acts as master controller for the hybrid system. MPC gives power references to wind and solar system local controllers based on the predicted load demands from the consumer side and under various constraints

Block Diagram of a Model Predictive Controller (shown in Fig 2.20):

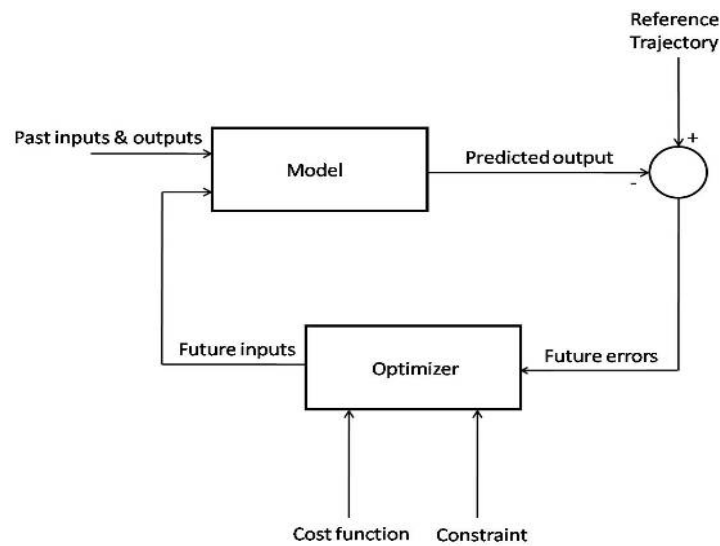


**Figure 2.20: Block Diagram of Model Predictive control**

## 2.10 Conclusion

Based on the extensive literature review on hybrid energy systems, including both solar and wind energy conversion systems. Following areas are considered for further investigation,

- Implementation of limited power point tracking for solar PV energy conversion system without using a battery at the DC bus.
- Implementation of limited power point tracking in wind energy conversion system without using a battery at the DC bus.
- Implementing the Model Predictive Controller for the solar & wind hybrid energy conversion system with power balancing as the objective function under various grid constraints.



# Chapter 3

## Limited Power Point Tracking For Grid-Connected SPVECS

Various topologies of the solar photovoltaic (SPV) system converter were discussed in previous chapter. This chapter deals with a two stage SPV energy conversion system that uses DC/DC buck converter as its first stage and a Voltage Source Inverter (VSI) as its second stage without the use of the battery at DC bus. In this chapter we will discuss in detail the SPV system Configuration, design, proposed control scheme for limited power point tracking using sliding mode control technique.

### 3.1 Solar power configuration

The system description, system modeling and proposed control scheme for limited power point tracking is presented in this section

#### 3.1.1 System description

In this research work, a Photovoltaic system with peak power capacity of 50kw is interfaced with three-phase three-wire grid with a shunt connected local load network. A two stage topology is implemented for interfacing PV system to the distribution network as shown in Figure 3.1. The first stage consists of a non isolated DC-DC buck converter. The main objective of power balancing is achieved through this buck converter. The buck converter operates in two operating regimes: i) when PV system output power is sufficient to supply the total load demand and ii) when PV system output power is insufficient to supply the load demand and the SPV system is at maximum power point. The control technique used for the converter to operate it in both the regime is sliding mode technique. A three-leg two-level voltage source

inverter (VSI) is used for transferring the power from PV panels to the point of common coupling (PCC) and to meet the reactive power requirement of the system if any. Current source inverter can also be used with the proposed control technique if and it will not affect the system as both the proposed sliding mode control of buck converter and the current control of inverter are independent of each other. Three inductors are used to interface the inverter with the grid. A shunt RC-filter is used as a ripple filter to remove high frequency ripple, which are caused due to high frequency switching of the inverter, from the PCC voltage. The SPV system and PV panel parameters are given in Table 3.1 & Table 3.2

**Table 3.1: SPVEC System Parameters**

C (output capacitance of buck converter)	11000 $\mu$ F
L (inductance of buck converter)	90 $\mu$ H
$f_{sw}$ (switching frequency of buck converter)	15 kHz
$L_{inf}$ (interfacing inductance)	5 mH
$V_{ll}$ (line to line grid voltage)	415V

**Table 3.2: The PV panel parameters**

PV Panel Parameters	
$N_s$ (number of PV cells in series)	1666
$N_p$ (number of pv cells in parallel)	22
q (charge of an electron)	$1.6 \times 10^{-19}C$
k (Boltzmann constant)	$1.3805 \times 10^{-23}Nm/K$
A (ideality factor)	1.60
K (PV cell's temperature coefficient)	$0.0017A/^{\circ}C$
$I_{scr}$ (PV cell short circuit current)	3.27A

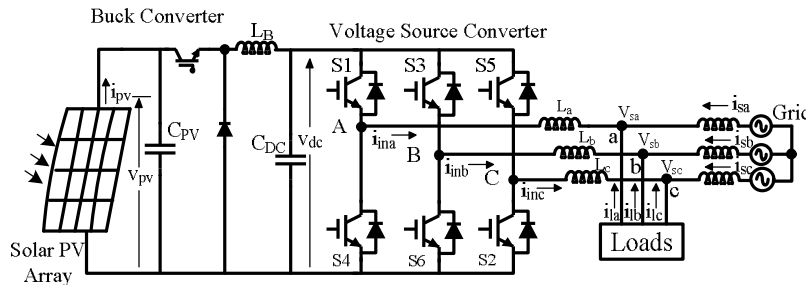




### Figure 3.1: SPV system Configuration

#### 3.1.2 System modeling

##### A. PV panel modeling

Double exponential model [38] of a photovoltaic cell is used for modelling the PV system. The PV cell is modelled as a current source given by equation (3.1)

$$I = I_{ph} - I_{s1} \left( e^{\frac{qV}{AKT}} - 1 \right) \quad (3.1)$$

where  $I_{ph}$  is the photo-generated current due to irradiation,  $I_{s1}$  is the reverse saturation current,  $V$  is the output voltage across the PV cell,  $I$  is the output current of the PV cell,  $k$  is the Boltzmann constant,  $T$  is the cell reference temperature,  $A$  is the ideality factor. The photo-generated current's ( $I_{ph}$ ) dependence on the irradiation ( $\lambda$ ) and cell temperature ( $T$ ) is modelled as follows.

$$I_{ph} = [I_{scr} + K(T - T_r)] \frac{\lambda}{100} \quad (3.2)$$

Where  $I_{scr}$  is the short circuit current of the PV cell,  $K$  is the short circuit current temperature coefficient,  $T_r$  is the cell reference temperature. The PV cell modules are connected in series and parallel combination to form the SPV system. The SPV system can be modelled using the following equation,(3.3)

$$I_{pv} = N_p I_{ph} - N_p I_{s1} \left( e^{\frac{qV_{pv}}{kTAN_s}} - 1 \right) \quad (3.3)$$

Where  $N_s$ ,  $N_p$  are the number of PV modules connected in series and parallel, respectively.  $I_{ph}$  is output current of the PV system and  $V_{pv}$  is the output voltage of the PV system. The SPV system is interfaced with a buck converter for power balancing. The buck converter modeling is explained in the next subsection.

##### B. Buck converter modeling

A nonlinear state space model of buck converter [39] is used here

$$\begin{aligned} \dot{V}_{pv} &= \frac{I_{pv}}{C} - \frac{I_0}{C} u \\ \dot{I}_0 &= -\frac{V_c}{L} + \frac{V_{pv}}{L} u \end{aligned} \quad (3.4)$$

Where the states  $I_o$  and  $V_{pv}$  are the output current and voltage of the buck converter, respectively. The input ( $u$ ) is 0 when the switch is OFF and 1 when the switch is ON. The non linear state space model is given as,

$$\dot{\mathbf{x}} = f(\mathbf{x}) + g(\mathbf{x})u \quad (3.5)$$

$$\text{Where, } \mathbf{x} = \begin{bmatrix} V_{pv} & I_o \end{bmatrix}^T, f(\mathbf{x}) = \begin{bmatrix} \frac{I_{pv}}{C} & -\frac{V_c}{L} \end{bmatrix}^T \text{ and } g(\mathbf{x}) = \begin{bmatrix} -\frac{I_o}{C} & \frac{V_{pv}}{L} \end{bmatrix}^T.$$

### 3.1.3 Control structure

The overall control structure of the proposed power balancing control strategy is shown in Figure 3.2. The entire control system is divided into three parts: i) sliding mode PV power control, ii) DC-link voltage control and iii) inverter current control. In the following subsections, each of these control systems is explained in detail

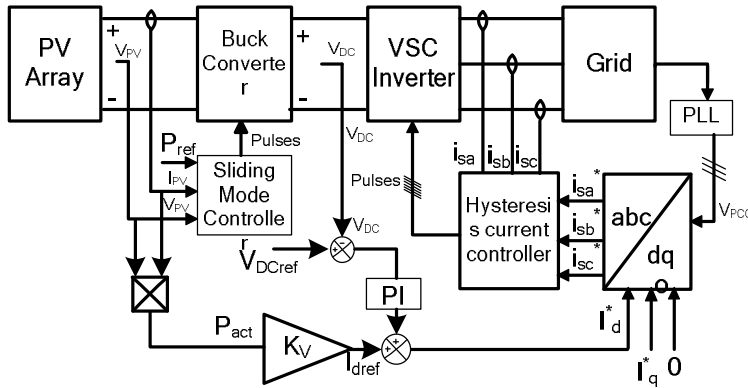


**Figure 3.2: the overall control system structure**

#### A. Sliding mode controller

The sliding mode control is a technique that maintains the system trajectory along a particular surface, which is commonly called a sliding regime or a sliding surface. A smoothing function ( $s(\mathbf{x})$ ), which reflects the dynamics of the sliding mode regime, is defined. A general control law for sliding mode control [40] can be represented by

$$u = \begin{cases} u^+ & \forall s(x) \geq 0 \\ u^- & \forall s(x) < 0 \end{cases} \quad (3.6)$$

where  $u^+$  and  $u^-$  are the control inputs to be applied whenever  $s(\mathbf{x})$  is nonzero

For the proposed sliding mode power-balancing controller, a smoothing function based on  $V_{pv}$  and  $I_{pv}$  is chosen. It is assumed here that the SPV system power output ( $P_{ref}$ ) is given and the sliding mode controller must maintain  $P_{ref}$ . For a distributed generation scenario, the SPV system may be getting the power generation set-point ( $P_{ref}$ ) either from a supervisory controller or  $P_{ref}$  may be decided based on a combination of load forecast and generation forecast.

Depending upon the instantaneous value of  $P_{ref}$  and maximum power generation capacity ( $P_{max}$ ) (which is dependent on the insolation level) of the SPV system, the buck converter is operated in one of the two modes: i) power sufficient mode (when  $P_{max} \geq P_{ref}$ ) and ii) power insufficient mode (when  $P_{max} < P_{ref}$ ). A variable structure control [45] is used for operating the buck converter in both the modes i.e. power sufficient mode and power insufficient mode. Thus during power sufficient mode, the SPV system must operate in LPPT mode and during power insufficient mode, the SPV system operate in MPPT mode. The propose control strategy provides such flexibility to operate in any of the two modes, depending on the load, climate conditions and status of the distributed generation system. Two different smoothing functions are chosen for the two modes of operation, as explained here

In power sufficient mode, the smoothing function  $s_1(\mathbf{x})$  is taken to be

$$s_1(\mathbf{x}) = P_{pv} - P_{ref} = 0 \quad (3.7)$$

where,  $P_{pv}$  is the instantaneous power output of the SPV System, given by  $V_{pv}^* I_{pv}$ . To achieve the sliding mode regime the transversality condition (3.8) has to be satisfied

$$L_g s_1 = \frac{\partial s_1}{\partial \mathbf{x}^T} g(\mathbf{x}) = -\frac{I_0 V_{pv}}{C} \left( \frac{\partial I_{pv}}{\partial V_{pv}} + \frac{I_{pv}}{V_{pv}} \right) \cong \frac{2I_0 I_{pv}}{C} \geq 0 \quad (3.8)$$

For the above transversality condition, the control law ( $u$ ) for power sufficient mode must be given as,

$$u = \begin{cases} 0 & \forall s_1(x) \geq 0 \\ 1 & \forall s_1(x) < 0 \end{cases} \quad (3.9)$$

When the buck converter is operating in power insufficient mode, another smoothing function  $s_2(\mathbf{x})$  is taken(3.10)

$$s_2(\mathbf{x}) = \left( \frac{\partial I_{pv}}{\partial V_{pv}} + \frac{I_{pv}}{V_{pv}} \right) = 0 \quad (3.10)$$

To achieve the sliding mode regime for  $s_2(\mathbf{x})$ , the following transversality condition has to be satisfied

$$L_g s_2 = \frac{\partial s_2}{\partial \mathbf{x}^T} g(\mathbf{x}) = -\frac{I_0}{CV_{pv}} \left( \frac{\partial I_{pv}}{\partial V_{pv}} + \frac{I_{pv}}{V_{pv}} \right) \quad (3.11)$$

$$\cong \frac{2I_0 I_{pv}}{CV_{pv}^2} \geq 0$$

For the above transversality condition the control law ( $u$ ) for power insufficient mode must be given as(3.12)

$$u = \begin{cases} 0 & \forall s_2(x) \geq 0 \\ 1 & \forall s_2(x) < 0 \end{cases} \quad (3.12)$$

When both the smoothing functions are combined, the complete sliding mode control algorithm can be obtained as,

$$u = \begin{cases} 0 & \forall s_1(x) \geq 0 \quad \& \quad P_{\max} \geq P_{ref} \\ 1 & \forall s_1(x) < 0 \quad \& \quad P_{\max} \geq P_{ref} \\ 0 & \forall s_2(x) \geq 0 \quad \& \quad P_{\max} < P_{ref} \\ 1 & \forall s_2(x) < 0 \quad \& \quad P_{\max} < P_{ref} \end{cases} \quad (3.13)$$

The output of the sliding mode controller ( $u$ ) will drive the buck converter as shown in Figure. 3.3. The actual power output of the SPV system ( $P_{act}$ ) is given by  $P_{act} = V_{pv} I_{pv}$ .

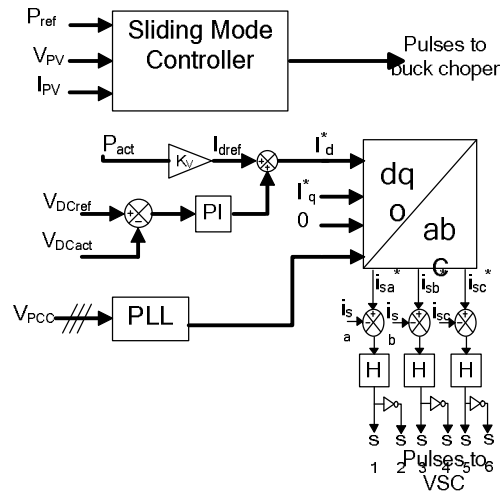


**Figure 3.3: the proposed Sliding mode control structure**

### B. DC Link voltage controller

For satisfactory operation of the inverter, the DC-link voltage should be maintained at a suitable voltage level, which is given by the following (3.14), [41,42,43]

$$V_{dc}^* = \frac{2\sqrt{2}V_{ll}}{\sqrt{3}m} \quad (3.14)$$

where,  $V_{ll}$  is the line to line voltage of the grid, and  $m$  is the modulation index. For the system parameters considered in this paper, the DC-link voltage should be maintained at 700V. In order to maintain this voltage level a PI-controller is used (Fig. 3.3). Reference DC-link voltage ( $V_{DC}^*$ ) is compared with actual DC-link voltage ( $V_{DC}$ ) and the error signal is given to the PI controller. The output of the PI controller determines current reference ( $I_d^*$ ) for the VSI

### C. Hysteresis current controller

Hysteresis current control technique is used to control the power flow through the inverter. The  $P_{act}$  coming from the SPV system is used to calculate the dq-frame current references ( $I_d^*$  and  $I_q^*$ ). The output from the PI controller of DC-link voltage controller is added to the  $I_{dref}$  obtained from the  $P_{act}$ . The final  $I_d^*$  and  $I_q^*$  (obtained from(3.15)), which are in dq0 reference frame (synchronous reference frame) are converted into abc frame (stationary reference frame) using a PLL(3.16).

$$I_d^* = I_{dref} + K_p \Delta V_{dc} + K_i \int \Delta V_{dc} dt \quad (3.15)$$

$$\begin{bmatrix} I_{sa}^* \\ I_{sb}^* \\ I_{sc}^* \end{bmatrix} = \frac{3}{2} \begin{bmatrix} \cos(\theta) & \cos(\theta - \frac{2\Pi}{3}) & \cos(\theta + \frac{2\Pi}{3}) \\ -\sin(\theta) & -\sin(\theta + \frac{2\Pi}{3}) & -\sin(\theta + \frac{2\Pi}{3}) \\ \frac{1}{2} & \frac{1}{2} & \frac{1}{2} \end{bmatrix} \begin{bmatrix} I_d^* \\ I_q^* \\ I_o^* \end{bmatrix} \quad (3.16)$$

The PLL synchronizes the inverter voltage with the grid voltage. The reference values thus obtained in stationary reference frame are subtracted from the instantaneous values of individual phase currents  $i_{sa}$ ,  $i_{sb}$ ,  $i_{sc}$  and then given to the hysteresis controllers operating with a band limit of (-0.2 A & 0.2 A). The output of this hysteresis controller is then given to relays, which will finally give the switching signals for inverter circuit. The controller parameters are given in Table 3.3.

**Table 3.3: DC link voltage and hysteresis controller Parameters**

$K_V$	0.0014
$K_p$	3
$K_i$	0.01
Band limit for Hysteresis control	-0.2 to 0.2

### 3.2 Simulation and Results

To demonstrate effectiveness and applicability of the proposed control strategy, simulations were carried out for various modes of operation. The simulation cases considered here are chosen to demonstrate the usefulness of the control algorithm under varying load demand as well as varying climate condition

#### Case-1: Sudden change in load demand

First simulations were carried out for variable load demand during power sufficient mode. Initially the SPV system was operating under steady state condition with load demand ( $P_{ref}$ ) of 30 kW when insolation level is 0.8 kW/m<sup>2</sup>. At this insolation level, the SPV system could generate a maximum power ( $P_{max}$ ) of 42 kW, indicating the sliding mode controller would be operating in power sufficient mode. At time  $t = 0.2$  sec, a step change from 30 kW to 20 kW in  $P_{ref}$  is given. Simulation results pertaining to the SPV power ( $P_{pv}$ ) output from the solar array, the voltage output of the buck converter ( $V_{dc}$ ), and inverter output current ( $i_a$ ) waveforms are shown in Figure 3.4. It can be observed from the waveforms that sliding mode controller responds very quickly to the set point change and the controller achieved desired power balance.

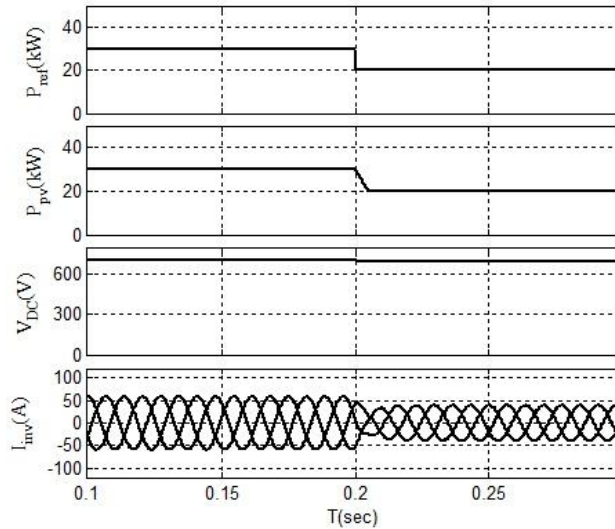


**Figure 3.4: Operating under step change in load demand**

### Case-2 : Operating in MPP mode

, the sliding mode controller's response to the power insufficient case is simulated. As in case-1, the system was initially operating under steady state condition with load demand ( $P_{ref}$ ) of 30 kW when insolation level is 0.8 kW/m<sup>2</sup>. At 0.2 sec  $P_{ref}$  was suddenly changed from 30 kW to 50 kW. As stated earlier, for insolation level of 0.8 kW/m<sup>2</sup>,  $P_{max}$  is 42 kW. Thus, the purpose of this simulation case is to demonstrate ability of the controller to move from power sufficient mode to power insufficient mode dynamically. Figure 5 shows response of the system to sudden increase in load demand and its effect on  $P_{pv}$ ,  $V_{dc}$ , and  $i_a$ . As can be seen from Figure 3.5, the sliding mode controller successfully switches from power sufficient mode to power insufficient mode and the system starts operating at MPP. As the power demand is more than  $P_{act}$ , the load network will draw remaining 8 kW power from the grid. It is important to note here that reactive power compensation can be also provided through VSI (CSI) in order to ensure only active power is drawn from the grid

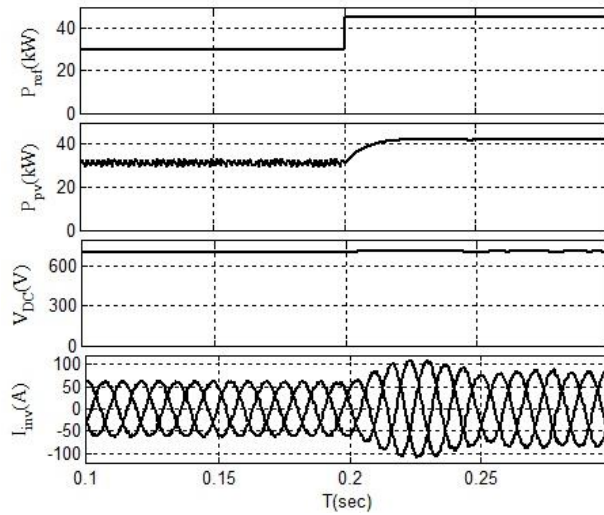


**Figure 3.5: Response during Power insufficient mode**

### Case-3: Sudden change in climatic conditions

SPV systems may often encounter sudden climate changes, which may sometime lead to system instability. In this case, simulations were carried out to study the effects of varying weather conditions by changing irradiation level. As in case-1, initially the system is operating at  $P_{ref} = 30$  kW, with  $\lambda = 0.8$  kW/m<sup>2</sup>. At 0.2 sec irradiation level was changed from 0.8 kW/m<sup>2</sup> to 0.6 kW/m<sup>2</sup>. As can be seen from Figure 3.6, the sliding mode controller performance is not affected by sudden climate change. In this case the controller was working in power sufficient mode during the simulation

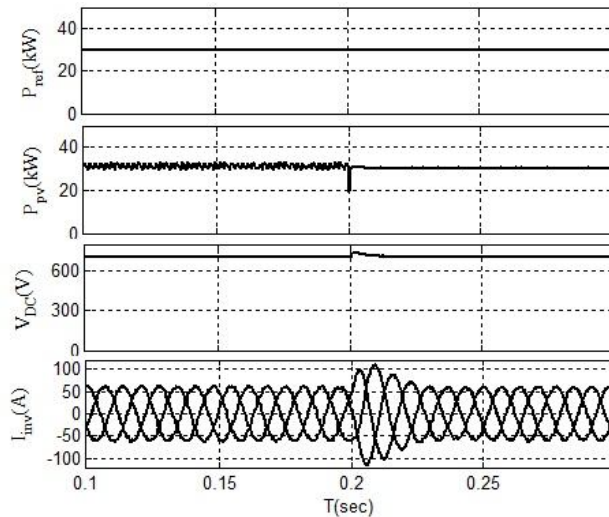


**Figure 3.6: Response to sudden change in climatic condition**



### Case 4: Islanded mode of operation

For grid-connected systems, there is always a possibility of going from grid-connected mode to islanded mode. The proposed control strategy would continue to work in islanded mode, as long as the system is operating in power sufficient mode. When the SPV system switches over from grid-connected mode to islanded mode, synchronization reference signal is also switched from grid reference to a pseudo reference signal available. In this case, simulations were carried out in islanded mode with initial load demand  $P_{ref} = 30$  kW, with  $\lambda = 0.8$  kW/m<sup>2</sup>. At 0.2 sec, the load demand was reduced from 30 kW to 10 kW. As can be seen from Fig.37, the sliding mode controller can operate in islanded mode as well. In this case, a voltage controlled VSI (as opposed to current controlled VSI used in earlier cases) was used to transfer power from the SPV system to the PCC. The sliding mode controller was working in power sufficient mode during the simulation. It must be noted here that in islanded mode, the system can deliver a maximum power of  $P_{max}$ . However, if load demand is higher than  $P_{max}$ , the supervisory controller must make appropriate decision to prevent system collapse

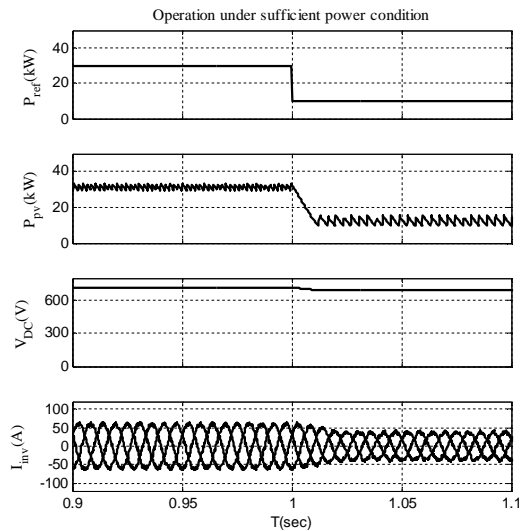


Figure 3.7: Response to load demand change during Islanded Mode

### 3.3 Conclusion

A power balancing sliding mode control strategy is proposed for grid-connected SPV systems. The main advantage of the proposed methodology is that back-up energy storage devices are not required for maintaining power balance and constant DC line voltage. Elimination of battery banks eliminates its maintenance and cost factor, this will improve overall SPV system power economy. The proposed sliding mode control algorithm can operate the buck converter in both the modes i.e. at maximum power point (power insufficient) and limited power point (power sufficient). The performance of the sliding mode controller demonstrated its effectiveness and applicability for grid-connected SPV systems under varying load and weather conditions.

# Chapter 4

## Limited Power Point Tracking For Grid-Connected WECS

As discussed in the Chapter-2, there are various topologies of the wind energy conversion system and turbines. In this chapter a full converter turbine that uses Permanent magnet Synchronous Generator (PMSG) as its generator without the use of battery at DC bus is studied and simulated. In this chapter, we will discuss in detail the wind power energy conversion system configuration, design, proposed control scheme for limited power point tracking using speed control of permanent magnet synchronous generator (PMSG).

### 4.1 Wind power configuration

The system description, system modeling and proposed control scheme for limited power point tracking is presented in this section.

#### 4.1.1 System description

In this chapter, a Wind energy conversion system with peak power capacity of 30kw is interfaced with the three phase three wire grid with a shunt connected local load network. A back to back AC/DC/AC topology is implemented for interfacing the WECS (Wind Energy Conversion System) to the distribution network as shown in Figure 4.1. The First stage consists of a controlled rectifier .The main objective of power balancing is achieved through the vector control technique of this controlled rectifier. The controlled rectifier operates in two operating region i) when WECS output power is sufficient to supply the total load demand ii) when WECS output power is insufficient

to supply the load demand and the WECS is at maximum power point. The control technique used for the controlled rectifier to operate in both the regions is speed control of PMSG through vector control. The reference point for speed of rotor ( $w_r^*$ ) is obtained based on the characteristics of wind turbine i.e. speed tip ratio ( $\lambda$ ), Power coefficient of wind turbine ( $C_p$ ) and the load demand at consumer site. A three-leg two-level voltage source inverter is used for transferring the power from WECS to the point of coupling (PCC) and to meet the reactive power if any. Current source inverter (CSI) can also be used with the proposed control technique and it will not affect the system as both the proposed control technique for Controlled rectifier and the current control of inverter are independent of each other. Three Inductors are used to interface the inverter with the grid. A shunt RC filter is used as a ripple filter to remove high frequency ripple, which are caused due to the high frequency switching of the inverter, from the PCC voltage. The WECS system parameters and Wind Turbine Parameters are given in Table 4.1 & Table 4.2.

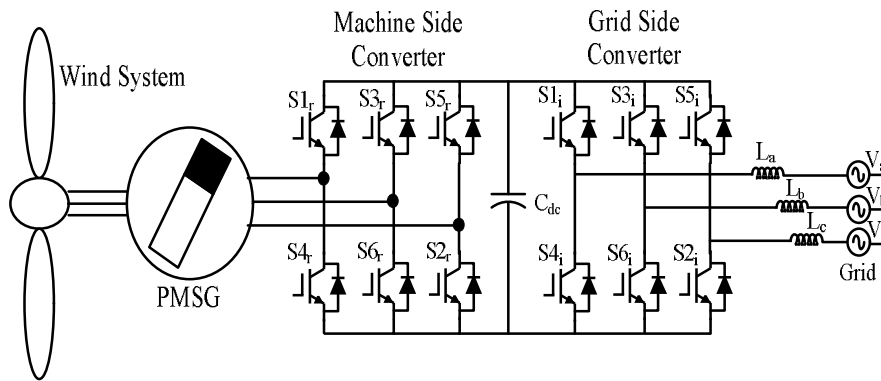


**Figure 4.1: WECS System Configuration**

**Table 4.1: WEC system Parameters**

C (output capacitance of controlled converter)	11000 $\mu$ F
L <sub>inf</sub> (interfacing inductance)	5 mH
V <sub>ll</sub> (line to line grid voltage)	415V

**Table 4.2: Wind turbine Parameters**

Performance Parameters	
Rated Electrical Power	30 kw
Wind speed cut- in	3 m/sec
Rated wind speed	10 m/sec
Rotor Parameters	
Type of Hub	Fixed Pitch
Rotor Diameter	15 m
Swept Area	177 m <sup>2</sup>
Rotor Speed@ rated wind	100 rpm
Generator Parameters	
Type	3 phase/6 pole synchronous
Voltage	680 V
kw @ Rated wind speed	30 kw
Speed RPM nominal	3000 rpm
Transmission Parameters	
Ratio	1 to 30 (rotor to gen speed)

#### 4.1.2 System modeling

##### A. Modeling of wind turbine with PMSG

Wind turbines cannot fully capture wind energy. The wind turbine model is based on three general equations [44]:

1. Equation for the extracted aero dynamical power (4.1)
2. Equation for the turbine power coefficient  $C_p$  (4.2)
3. Equation for the tip speed ratio  $\lambda$  (4.3)

The model has three inputs: the wind speed, the pitch angle and the rotor speed

$$P_{wind} = \frac{1}{2} \rho A v_w^3 C_p(\lambda, \beta) \quad (4.1)$$

$$C_p = a_1 \left( \frac{a_2}{\lambda_i} - a_3 \beta - a_4 \right) e^{-\frac{a_5}{\lambda_i}} \quad (4.2)$$

$$\lambda = \frac{w_r R}{v_w} \quad (4.3)$$

Where  $\rho$  is the air density is equal to  $1.225 \text{ kg/m}^3$ ,  $A$  is the area swept by the blade,  $v_w$  is the wind speed and  $C_p$  is the power coefficient which depends on the tip speed ratio (4.3) and  $\beta$  is the pitch angle,  $R$  radius of the blade. Variation of  $C_p$  with the change in tip speed ratio  $\lambda$  keeping pitch angle  $\beta = 0$  is shown Figure 4.2

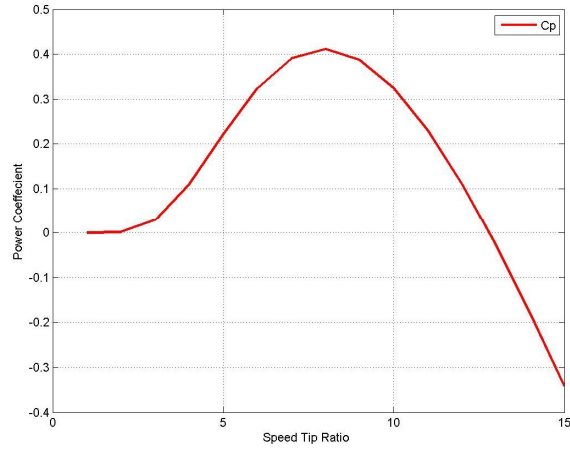


**Figure 4.2:  $C_p$  (Power Coefficient) Vs  $\lambda$  (Speed tip Ratio)**

It can be observed from the Fig 4.2 that Power extracted by any wind turbine from the wind energy is the only 41% of the maximum energy available from the wind normally. For the aim of this study the pitch angle is kept to 0 as no pitch angle control is considered in this study of work.

The rotor speed input is connected to the one mass mechanical drive train model computing the turbine rotor swing. The equation is [45] :

$$(J_T + J_G) \frac{dw_g}{dt} = T_T - T_G - Dw_g \quad (4.4)$$

Where  $J_T$  and  $J_G$  are the turbine and generator moment of inertia,  $T_T$  and  $T_G$  are the turbine and electromagnetic torque,  $D$  is the viscous friction factor and  $w_g$  is the generator rotor speed.

## B. PMSG model

Dynamic modelling of PMSG can be described in d-q reference system as follows [46]:

$$\frac{di_q}{dt} = -\frac{r_s}{L}i_q - w_e i_d + \frac{w_e \Phi_m}{L} - \frac{V_{gq}}{L} \quad (4.5)$$

$$\frac{di_d}{dt} = -\frac{r_s}{L}i_d + w_e i_q - \frac{V_{gd}}{L} \quad (4.6)$$

$$w_e = p w_g \quad (4.7)$$

$$T_e = -\frac{3}{2} p \Phi_m i_q \quad (4.8)$$

Where  $r_s$  is the stator resistance,  $L$  is the inductance of the generator on the  $d$  and  $q$  axis which are taken to be equal,  $\Phi_m$  is the permanent magnetic flux and  $w_e$  is the electrical rotating speed of the generator defined by equation (4.7) and  $p_n$  are the number of pole pairs. In order to complete the modeling of PMSG the output electromagnetic torque  $T_e$  can be described by (4.8) when direct axis current  $i_d$  is kept zero.

### 4.1.3 Control structure

The overall control structure of the proposed power balancing control strategy is shown in Figure 4.3. The entire control system is divided into three parts: i) Limited Power Point Tracking (LPPT) Control of PMSG using vector control technique for controlled rectifier, ii) DC-link Voltage control and iii) inverter current control. In the following subsections, each of these control system is explained in detail.

#### A. Limited power point control

The proposed control technique is based on the characteristics curve between the  $C_p$  (power coefficient) and  $\lambda$  (speed tip ratio) shown in Fig 4.2 for obtaining the required reference speed of the rotor based on the load demand. We will be operating the controller on the left hand side of the characteristics curve of  $C_p$  and  $\lambda$  because if we operate it on the right hand side of the curve, speed of the rotor will increase more than the rated speed of generator thereby increasing the mechanical stresses on the

generator. The mathematical relation between  $P_{ref}$  (Power Reference/Load Demand) and  $w_{ref}$  (speed of the rotor) required to generate that much Load demand  $P_{ref}$  are given by following equation:

$$C_{pref} = \frac{P_{ref}}{P_{max}} \quad (4.9)$$

$$\lambda_{ref} = 12.28C_p + 2.5 \quad (4.10)$$

$$w_{ref}^* = \frac{\lambda_{ref} v_w}{R} \quad (4.11)$$

$$P_{max} = \frac{1}{2} \rho A v_w^3 \quad (4.12)$$

$C_{pref}$  In equation (4.9) gives the desired power coefficient for the wind turbine based on the load demand ( $P_{ref}$ ). Equation (4.10) is obtained by approximating the left hand side of the curve to approximately a linear straight line and adding an offset to compensate for the linear approximation of the curve. The desired reference speed then can be obtained from the relation given by equation(4.11).

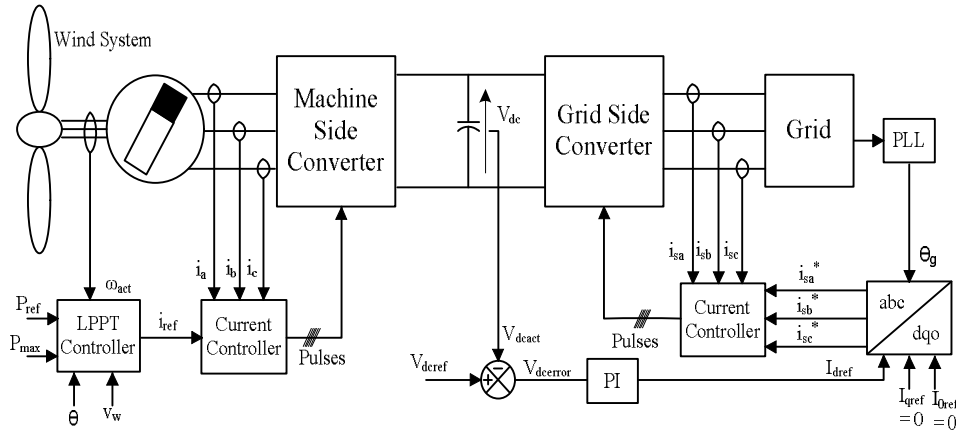


**Figure 4.3: Overall control system structure**

## B. Speed control of PMSG

Field oriented control strategy is implemented in the synchronous rotating reference frame for an easier control. The control strategy requires three controllers, two for the



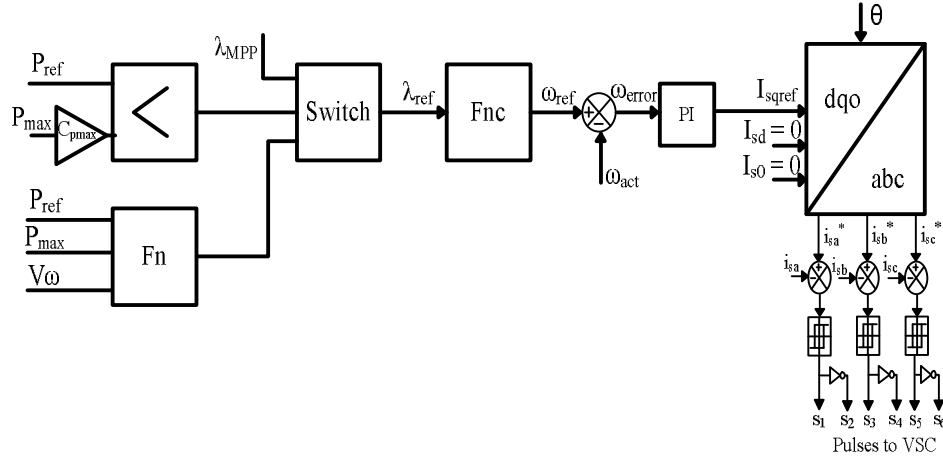
currents in the inner loop and one for the outer loop. An important requirement is that the current controllers must react faster on the input variations than the speed controller. The field oriented Control schematic block is represented in Figure 4.4.

For implementing the strategy in Figure 4.4 the acquisition of the three phase stator currents, the DC link voltage and the rotor position are required. It is not necessary to monitor all three stator currents  $i_{sa}, i_{sb}, i_{sc}$ . It is sufficient to use only two current sensors because the sum of the three phase current is always zero. The speed of the rotor  $\omega_g$  can be measured through the speed sensors which can then be integrated to obtain rotor position. Knowing the rotor position  $\theta_g$  the park coordinate transformation is applied to the current references  $i_{sqref}, i_{sdref}$ , thus obtaining  $i_{sa}^*, i_{sb}^*, i_{sc}^*$  references in stationary reference frame coordinates.

Hysteresis current controller is used to generate the PWM (Pulse Width Modulation) signals. The reference values thus obtained from the speed PI controller of the outer loop in stationary reference frames are subtracted from the instantaneous values of individual phase currents  $i_{sa}, i_{sb}, i_{sc}$  and then given to hysteresis controllers operating with a band limit of (-0.1A & 0.1 A). The output of this hysteresis controller is then given to relays, which will finally give the switching signals for rectifier circuit. The controller parameter are given in Table 4.3

**Table 4.3: LPPT controller parameters**

$C_{pmax}$	0.41
$K_p$	12
$K_i$	0.234
Band limit for Hysteresis control	-0.1 to 0.1



\* Fn is equation-(4.10)

\*Fnc is equation-(4.11)

Figure 4.4: Proposed LPPT controller

### C. DC Link voltage controller

For satisfactory operation of the inverter, the DC-link voltage should be maintained at a suitable voltage level which is given by the following [46]

$$V_{dc}^* = \frac{2\sqrt{2}V_{ll}}{\sqrt{3}m} \quad (4.13)$$

Where  $V_{ll}$  is the line to line voltage of the grid, and  $m$  is the modulation index. For the system parameters considered in this paper, the voltage should be maintained at 700V. In order to maintain this voltage level a PI controller is used in the Figure 4.3. Reference DC link voltage ( $V_{dc}^*$ ) is compared with actual DC-Link voltage ( $V_{dc}$ ) and the error signal is given to the PI controller. The output of the PI controller determines current references ( $I_d^*$ ) for the VSI.

### D. Inverter controller

Hysteresis current control technique is used to control the power flow through the inverter. The  $P_{act}$  coming from the WECS is used to calculate the dq –frame current references ( $I_d^*$  and  $I_q^*$ ). The output from the PI controller of DC-link Voltage controller is added to the  $I_{dref}$  obtained from  $P_{act}$ . The final  $I_d^*$  and  $I_q^*$  obtained from equation (4.14) which are in dq0 reference frame (synchronous reference frame) are converted into abc frame (stationary reference frame) using PLL (4.15).

$$I_d^* = I_{dref} + K_p \Delta V_{dc} + K_i \int \Delta V_{dc} dt \quad (4.14)$$

$$\begin{bmatrix} I_{sa}^* \\ I_{sb}^* \\ I_{sc}^* \end{bmatrix} = \frac{3}{2} \begin{bmatrix} \cos(\theta) & \cos(\theta - \frac{2\Pi}{3}) & \cos(\theta + \frac{2\Pi}{3}) \\ -\sin(\theta) & -\sin(\theta + \frac{2\Pi}{3}) & -\sin(\theta + \frac{2\Pi}{3}) \\ \frac{1}{2} & \frac{1}{2} & \frac{1}{2} \end{bmatrix} \begin{bmatrix} I_d^* \\ I_q^* \\ I_o^* \end{bmatrix} \quad (4.15)$$

The PLL synchronises the inverter voltage with the grid voltage. The reference values thus obtained in stationary reference frame are subtracted from the instantaneous values of individual phase currents  $i_{ga}, i_{gb}, i_{gc}$  and then given to hysteresis controllers operating with a band limit of (-0.1A & 0.1 A). The output of this Hysteresis controller is then given to relays, which will finally give the switching signals for rectifier circuit. The controller Parameters are given in Table 4.4.

**Table 4.4: DC link voltage and hysteresis controller parameters**

$K_v$	0.0014
$K_p$	3
$K_i$	0.01
Band limit for Hysteresis control	-0.1 to 0.1

## 4.2 Simulation and Results

The proposed wind energy conversion system was designed and modelled in MATLAB Simulink using Simpowersystem blocks. To demonstrate effectiveness and applicability of the proposed control strategy, simulations were carried out for various modes of operation. The simulation cases considered here are chosen to demonstrate the usefulness of the control algorithm under varying load demand as well as varying climate conditions

**Case 1: Sudden change in load demand**

First simulations were carried out for variable load demand during power sufficient mode. Initially the WECS system was operating under steady state condition with load demand ( $P_{ref}$ ) of 15 kw when wind speed is 9 m/sec .At this wind speed the WECS can generate a maximum power ( $P_{max}$ ) of 30 kw, indicating that the proposed control technique will be operating in power sufficient mode. At time t=1 sec, a step change from 15 kw to 25 kw in  $P_{ref}$  is given. Simulation results pertaining to the WECS power ( $P_{act}$ ) output from the wind turbine,  $V_{dc}$  dc link voltage,  $w_{ref}$  reference speed of generator in rads/sec,  $w$  actual speed of the generator, and inverter output current ( $i_{abc}$ ) waveforms are shown in Figure 4.5. It can be observed from the waveforms that the proposed controller responds very quickly to the set point changes and the controller achieved the power balance.

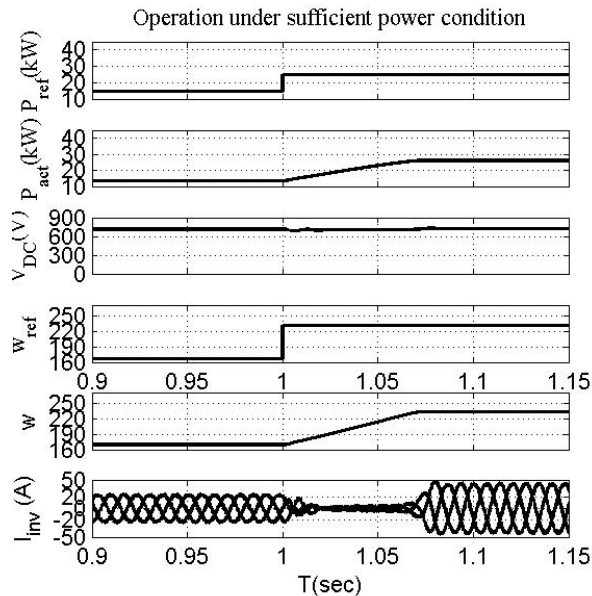


**Figure: 4.5 Response to a step change in load demand**

**Case 2: Operation in MPP mode**

Next, the proposed controller's response to the power insufficient case is simulated. As in case-1, the system was initially operating under steady state condition with load demand ( $P_{ref}$ ) of 15 kw when wind speed is 9 m/sec .At 1 sec  $P_{ref}$  was suddenly changed from 15 kw to 40 kw .As stated earlier, for wind speed of 9 m/sec,  $P_{max}$  is 30 kw. Thus the purpose of this simulation case is to demonstrate ability of the controller to move from power sufficient mode to power insufficient mode dynamically. Figure 4.6 shows response of the system to sudden increase in load demand and its effect on  $P_{act}$ ,  $V_{dc}$ ,  $w$  and  $i_{abc}$ . AS can be seen the controller successfully switches from power sufficient mode to power insufficient mode and the system starts operating at MPP. As the power demand is more than the  $P_{act}$ , the load network will draw remaining 10 kw from the grid.

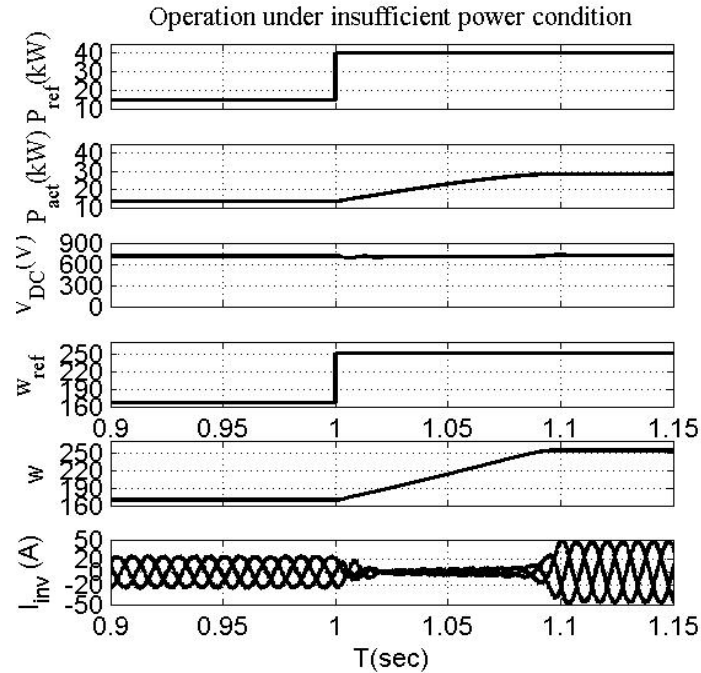


**Figure: 4.6 Operation under insufficient power condition**

### Case 3: Sudden change in climatic conditions

WECS systems often encounter sudden climatic changes, which may sometimes lead to system instability. In this case simulations were carried out to study the effects of varying weather conditions by changing wind speed. The system is initially operating at  $P_{ref} = 25$  kW, with wind speed 9 m/sec. At  $t = 1$  sec the wind speed is changed from 9 m/sec to 8 m/sec. At 8 m/sec the  $P_{max} = 20$  kW. As can be seen from Figure 4.7, the controller performance is not affected. In this case the controller shifts from sufficient mode to insufficient mode during the simulation.

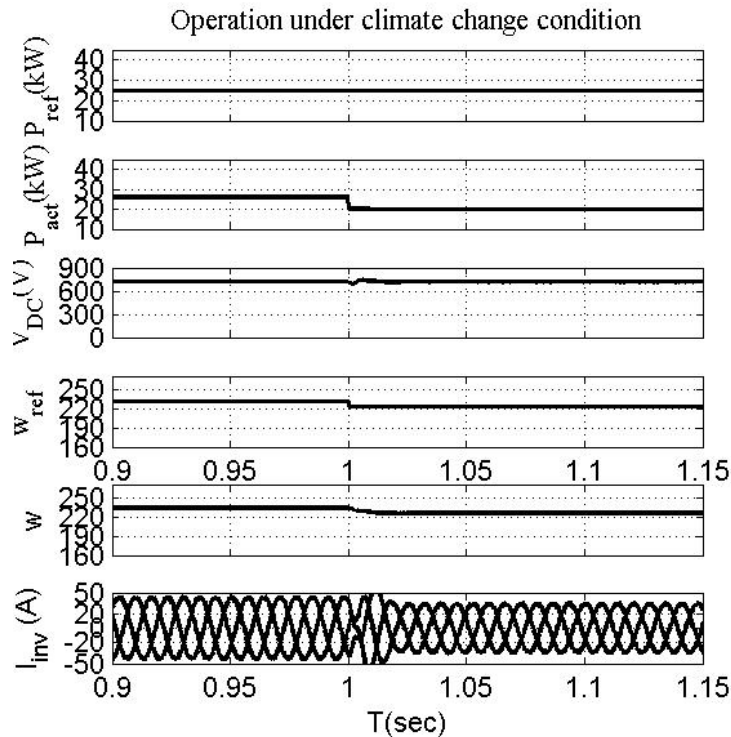


Figure: 4.7 Operation under sudden climate change condition

### 4.3 Conclusion

A power balancing limited power point control strategy is proposed for grid-connected WEC systems. The main advantage of the proposed methodology is that back-up energy storage devices are not required for maintaining power balance and constant DC line voltage. Elimination of battery banks eliminates its maintenance and cost factor, this will improve overall WECS system power economy. The proposed limited power point control algorithm can operate the controlled converter in both the modes

i.e. at maximum power point (power insufficient) and limited power point (power sufficient). The performance of the limited power point controller demonstrated its effectiveness and applicability for grid-connected WEC systems under varying load and weather conditions.

# Chapter 5

## MPC implementation of HECS

As discussed in the Chapter-2, to make the system more reliable and efficient, the limited power point tracking operating points for LPPT controllers can be optimised based on the future predictions of load demand, solar irradiation predictions, wind speed predictions, operating costs of solar and wind. In this chapter we will discuss the model predictive control implementation for solar, wind energy conversion system, overall control architecture and its implementation for hybrid energy conversion system.

### 5.1 Model predictive control

Model predictive control is an effective means of dealing with multivariable constrained problems. Predictive control is a class of control strategies based on the explicit use of a process model to generate the predicted values of the output at future time instants, which are then used to compute a sequence of control moves that optimize the future behavior of a plant. Predictive control is rather a methodology than a single technique. The difference in the various methods is mainly the way the problem is translated into mathematical formulation.

All the model predictive controllers (MPC) algorithms possess common elements, and different options can be chosen for each element giving rise to different algorithms.

These elements are:

- Prediction model
- Objective function and
- Obtaining the control law

#### 5.1.1 Prediction Model



The models can be Impulse/step response models, transfer function models or state space models.

**Impulse response model:** It is known as weighting sequence or convolution model. The output is related to the input by the equation

$$y(t) = \sum_{i=1}^{\infty} h_i u(t-i) \quad (5.1)$$

Where  $h_i$  is the sampled output when the process is excited by a unitary impulse. This sum is truncated and only  $N$  values are used

$$y(t) = \sum_{i=1}^N h_i(t) u(t-i) = H(z^{-1})u(t) \quad (5.2)$$

Where  $z^{-1}$  is the backward shift operator, the prediction will be given by

$$\hat{y}(t+k|t) = H(z^{-1})u(t+k|t) \quad (5.3)$$

This method is widely used in the industrial practice. The model is easily obtained by rather simple experiments and gives good results. The disadvantage is that it requires a large amount of parameters.

**Step response model:** It is very similar to impulse except that the input signal is a step. For stable systems, the truncated response is given by:

$$y(t) = y_0 + \sum_{i=1}^N g_i \square u(t-i) = y_0 + G(z^{-1})(1-z^{-1})u(t) \quad (5.4)$$

Where  $g_i$  are the sampled output values for the step input and  $\square u(t) = u(t) - u(t-1)$ ,

$$h_i = g_i - g_{i-1}.$$

Model has the same advantage and disadvantage as that of impulse response method.

**Transfer function model:** This uses the concept of transfer  $G = B/A$  so that the output is given by

$$A(z^{-1})y(t) = B(z^{-1})u(t) \quad (5.5)$$

Thus the prediction model is given by

$$\hat{y}(t+k|t) = \frac{B(z^{-1})}{A(z^{-1})} u(t+k|t) \quad (5.6)$$

This representation is valid for unstable processes also and the advantage of this method is that it requires few parameters, although prior knowledge of process is necessary, especially that of the order of A and B polynomials.

**State space models:** It has the following representation

$$\begin{aligned}x(t) &= Ax(t-1) + Bu(t-1) \\y(t) &= Cx(t)\end{aligned}\tag{5.7}$$

Where  $x$  is the state and  $A, B, C$  are the matrices for system, input, output respectively. The prediction for this model is given by

$$\hat{y}(t+k|t) = C \hat{x}(t+k|t) = C \left[ A^k x(t) + \sum_{i=1}^k A^{i-1} Bu(t+k-i|t) \right]\tag{5.8}$$

It has the advantage that it can be used for multivariable processes in a straight forward manner. The control law is simply the feedback of linear combination of the state vector, although sometimes the state basis has no meaning. The calculations may be complicated with the additional necessity of including an observer if the states are not accessible.

### 5.1.2 Objective function

The various MPC algorithms propose different cost functions for obtaining the control law. The general aim is that the future output ( $y$ ) on the considered horizon should follow a determined reference signal ( $w$ ) and, at the same time, the control effort ( $\Delta u$ ) necessary for doing so should be penalised. The generalized expression for such an objective function will be:

$$J(N1, N2, N3) = \sum_{j=N1}^{N2} \left[ \hat{y}(t+j|t) - w(t+j) \right]^2 R + \sum_{j=1}^{N3} \left[ \Delta u(t+j|t) \right]^2 Q\tag{5.9}$$

It is a quadratic function with  $u(t+j)$  is the future inputs, and the error between the future values of reference output  $w(t+j)$  and predicted outputs  $\hat{y}(t+j|t)$ . Weights  $R$  and  $Q$  are used to adjust the error and the inputs respectively.  $N2 - N1$  is the prediction horizon,  $N3$  is the control horizon.

In practice all the processes are subject to constraints. The actuators have a limited field of action and a determined slew rate, as is the case of the valves. This makes the introduction of constraints in the function to be minimized necessary.

### 5.1.3 Obtaining the control law

In order to obtain  $u(t+k|t)$  it is necessary to minimize the functional  $J$  of equation (5.9) . To do this the values of the predicted outputs  $\hat{y}(t+k|t)$  are calculated as a function of past values of inputs and outputs and future control signals, making use of prediction model chosen and substituted in the cost function, obtaining an expression whose minimization leads to the looked for values.

### 5.1.4 Model predictive control algorithms

- Dynamic Matrix Control: This control uses step response model (5.4) .
- Model Algorithmic Control: This control uses impulse response model(5.3)
- Generalized Predictive Control: This control uses CARIMA model based on (5.6)

## 5.2 Model predictive control implementation for solar energy conversion system

The linearized state space model of the nonlinear solar photovoltaic system is obtained. This state space model is used for obtaining prediction model for MPC controller. Receding horizon control algorithm is used for MPC controller. In Receding horizon control scheme the prediction values used for reference output can be any value greater than 2 but the predicted control move used is always for the next sampling time only.

### 5.2.1 Control architecture for solar energy conversion system

The control algorithm has a two stage hierarchal architecture. First stage is a master controller based on MPC and second stage is a local controller which is based on sliding mode control. Master controller (MPC) calculates the optimized reference power point based on future load predictions and various constraints for the local controller (LPPT). LPPT controller then operates either in LPPT or MPPT depending on the reference point set by MPC and the maximum power that can be generated by solar system. Control architecture is shown in Figure 5.1.

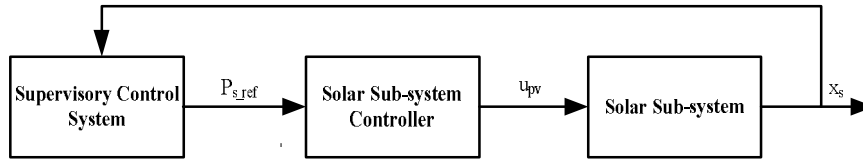


**Figure 5.1 Control architecture for solar energy conversion system**

### 5.2.2 Linearized state space model for solar photovoltaic energy conversion system

Averaged Non linear state space model for SPV system is given by:

$$\begin{aligned} \frac{\partial V_{pv}}{\partial t} &= \frac{i_{pv}}{C_{pv}} - \frac{i_o}{C_{pv}} D \\ \frac{\partial i_o}{\partial t} &= -\frac{V_{dc}}{L_B} + \frac{V_{pv}}{L_B} D \end{aligned} \quad (5.10)$$

Where  $V_{pv}$  is voltage across PV module,  $i_o$  is the output current of buck converter,  $V_{dc}$  is the output dc voltage of buck converter,  $D$  is the duty ratio of buck converter.

For buck converter  $V_{out} = DV_{in}$ , the sliding mode controller will always operate on the right hand side of the power vs. voltage characteristic of Solar PV module shown in Figure 5.2

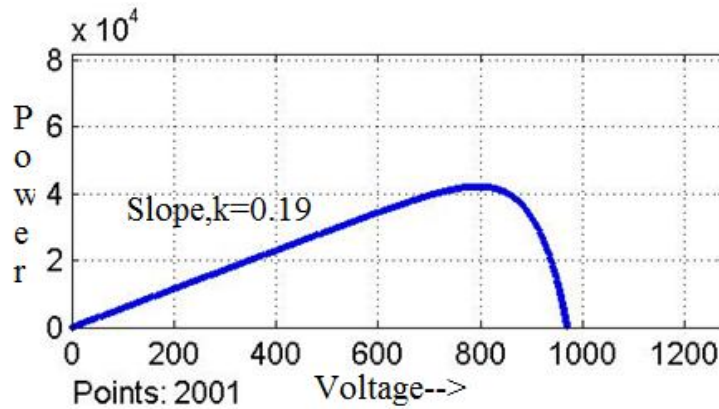


**Figure 5.2 PV characteristic of solar module**

So,  $V_{in} = kP_{ref}$ ,  $V_{DC} = DkP_{ref}$ , therefore nonlinear averaged state space model in terms of  $P_{ref}$  as an input decision variable is given by

$$\begin{aligned}\frac{\partial V_{pv}}{\partial t} &= \frac{i_{pv}}{C_{pv}} - \frac{i_o}{C_{pv}} \left[ \frac{V_{DC}}{kP_{ref}} \right] \\ \frac{\partial i_o}{\partial t} &= -\frac{V_{dc}}{L_B} + \frac{V_{pv}}{L_B} \left[ \frac{V_{DC}}{kP_{ref}} \right]\end{aligned}\quad (5.11)$$

This nonlinear state space model is linearised using Jacobian linearization technique and then it is used for state space prediction model.

**Linearized state space thus obtained will be of form:**

$$\begin{aligned}\dot{[x]} &= A[x] + B[u] \\ [w] &= C[x]\end{aligned}$$

Where  $x = [V_{pv} \quad i_o]^T$ ,  $u = [P_{sref}]$ ,  $w = P_{out}$  is the instantaneous power produced by SPVECS,  $\hat{y}$  load demand predictions

**Objective function is:**

$$J(0, 2, 1) = \sum_{j=0}^2 \|\hat{y}(t+j|t) - w(t+j)\|^2 R + \sum_{j=1}^1 \|\Delta u(t+j|t)\|^2 Q$$

### 5.2.3 Simulation and Results

Simulation was carried out for variable demand predictions over 250 samples. Initially the solar system is operated under steady state condition with load demand of 10 kw for fixed solar irradiation of 0.8 pu. The weights  $R$  and  $Q$  are set to 1900 and 33 respectively. Figure 5.3 shows the tracking of  $P_{ref}$  the input decision variable with the  $w$  predicted output. Prediction horizon is chosen to be 2 and control horizon is chosen to be 1. Sampling time is chosen to be 0.1

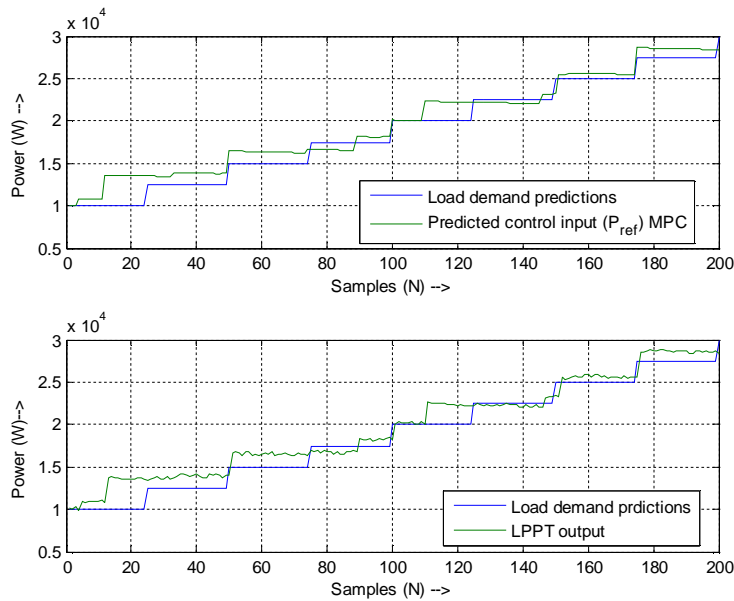


**Figure 5.3 Model predictive control implementation of solar energy conversion system**

### 5.3 Model predictive control implementation of wind energy conversion system

The linearized state space model of the nonlinear wind energy system is obtained. This state space model is used for obtaining prediction model for MPC controller. Receding horizon control algorithm is used for MPC controller. In Receding horizon control scheme the prediction values used for reference output can be any value greater than 2 but the predicted control move used is always for the next sampling time only.

#### 5.3.1 Control architecture for wind energy conversion system

The control algorithm has a two stage hierarchal architecture. First stage is a master controller based on MPC and second stage is a local controller which is based on sliding mode control. Master controller (MPC) calculates the optimized reference power point based on future load predictions and various constraints for the local controller (LPPT). LPPT controller then operates either in LPPT or MPPT depending on the reference point set by MPC and the maximum power that can be generated by solar system. Control architecture is shown in Figure 5.4.

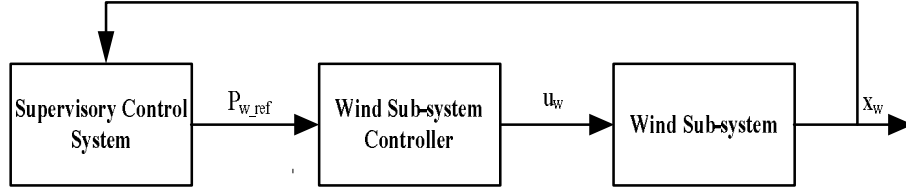


Figure 5.4: Control architecture for wind energy conversion system

### 5.3.2 Linearized state space model for wind energy system

Average non linear state space model for WECS is given by:

$$\begin{aligned}
 \frac{di_q}{dt} &= -\frac{R_s}{L}i_q - w_e i_d + \frac{w_e \Phi_m}{L} - \frac{\Pi V_{dc}^2 i_{qref}}{3\sqrt{3}P_e} \\
 \frac{di_d}{dt} &= -\frac{R_s}{L}i_d + w_e i_q \\
 \frac{dw_e}{dt} &= \frac{P}{2J} \left( T_m - \frac{3P}{4} \Phi_m i_q \right) \\
 \frac{di_{qref}}{dt} &= \frac{K_p K}{P_{max}} - \frac{K_p P T_m}{2J} + \frac{3P^2 K_p \Phi_m i_q}{8J} + \frac{K_i K P_{ref}}{P_e} - K_i w_e
 \end{aligned} \tag{5.12}$$

Where  $i_q, i_d, w_e, i_{qref}$  are the states and  $P_{ref}$  is the control input for mpc.

This nonlinear state space model is linearised using Jacobian linearization technique and then it is used for state space prediction model.

**Linearized state space thus obtained will be of form:**

$$\begin{aligned}
 \dot{[x]} &= A[x] + B[u] \\
 [w] &= C[x]
 \end{aligned}$$

Where  $x = [i_q \ i_d \ w_e \ i_{qref}]^T, u = [P_{wref}]$ ,  $w = P_{out}$  is the instantaneous power produced by WECS,  $\hat{y}$  load demand predictions

**Objectivefunction is:**

$$J(0,3,1) = \sum_{j=0}^3 \|\hat{y}(t+j|t) - w(t+j)\|^2 R + \sum_{j=1}^1 \|\Delta u(t+j|t)\|^2 Q$$

### 5.3.3 Simulation and Results

Simulation was carried out for variable demand predictions over 20 samples. Initially the wind system is operated under steady state condition with load demand of 10 kw for fixed wind speed of 8m/sec. The weights  $R$  and  $Q$  are set to 200 and 12 respectively. Figure 5.5 shows the tracking of  $P_{ref}$  the input decision variable with the  $w$  predicted output. Prediction horizon is chosen to be 3 and control horizon is chosen to be 1. Sampling time is chosen to be 0.5

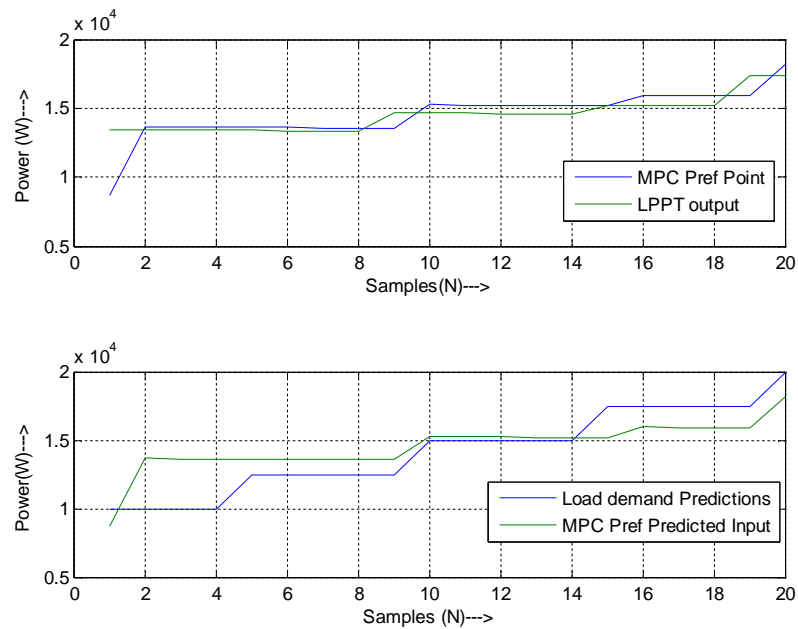


**Figure 5.5: Model predictive control implementation of wind energy conversion system**

#### 5.4 MPC implementation of hybrid energy conversion system (HECS)

Overall architecture for HECS is shown in Figure 5.6



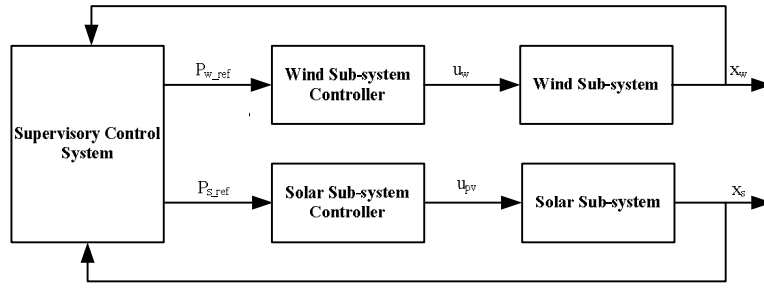


Figure 5.6: Control architecture for HECS

Averaged nonlinear state space model of the system becomes:

$$\begin{aligned}
 \frac{\partial V_{pv}}{\partial t} &= \frac{i_{pv}}{C_{pv}} - \frac{i_o}{C_{pv}} \left[ \frac{V_{DC}}{kP_{sref}} \right] \\
 \frac{\partial i_o}{\partial t} &= -\frac{V_{dc}}{L_B} + \frac{V_{pv}}{L_B} \left[ \frac{V_{DC}}{kP_{sref}} \right] \\
 \frac{di_q}{dt} &= -\frac{R_s}{L} i_q - w_e i_d + \frac{w_e \Phi_m}{L} - \frac{\Pi V_{dc}^2 i_{qref}}{3\sqrt{3}P_e} \\
 \frac{di_d}{dt} &= -\frac{R_s}{L} i_d + w_e i_q \\
 \frac{dw_e}{dt} &= \frac{P}{2J} \left( T_m - \frac{3P}{4} \Phi_m i_q \right) \\
 \frac{di_{qref}}{dt} &= \frac{K_p K}{P_{max}} - \frac{K_p P T_m}{2J} + \frac{3P^2 K_p \Phi_m i_q}{8J} + \frac{K_t K P_{wref}}{P_e} - K_i w_e
 \end{aligned} \tag{5.13}$$

This nonlinear state space model is linearised using Jacobian linearization technique and then it is used for state space prediction model.

Linearized state space thus obtained will be of form:

$$\begin{aligned}
 \dot{[x]} &= A[x] + B[u] \\
 [w] &= C[x]
 \end{aligned}$$

Where  $x = [V_{pv} \quad i_o \quad i_q \quad i_d \quad w_e \quad i_{qref}]^T$ ,  $u = \begin{bmatrix} P_{sref} \\ P_{wref} \end{bmatrix}$ ,  $w = P_{out}$  is the instantaneous

power produced by HECS,  $\hat{y}$  load demand predictions

**Objective function is:**

$$J(0, 2, 1) = \sum_{j=0}^2 \hat{y}(t+j|t) - w(t+j)^2 R + \sum_{j=1}^1 \Delta u(t+j|t)^2 Q$$

### 5.4.1 Simulation and Results:

Simulation was carried out for variable demand predictions over 20 samples. Initially the HECS system is operated under steady state condition with load demand of 20 kw for fixed wind speed of 8m/sec, solar irradiation of 0.8pu. The weights  $R$  and  $Q$  are set to 500 and [0.00001 1] respectively. Figure 5.7 shows the tracking of  $P_{ref}$  the input decision variable with the  $w$  predicted output. Prediction horizon is chosen to be 3 and control horizon is chosen to be 1. Sampling time is chosen to be 0.5

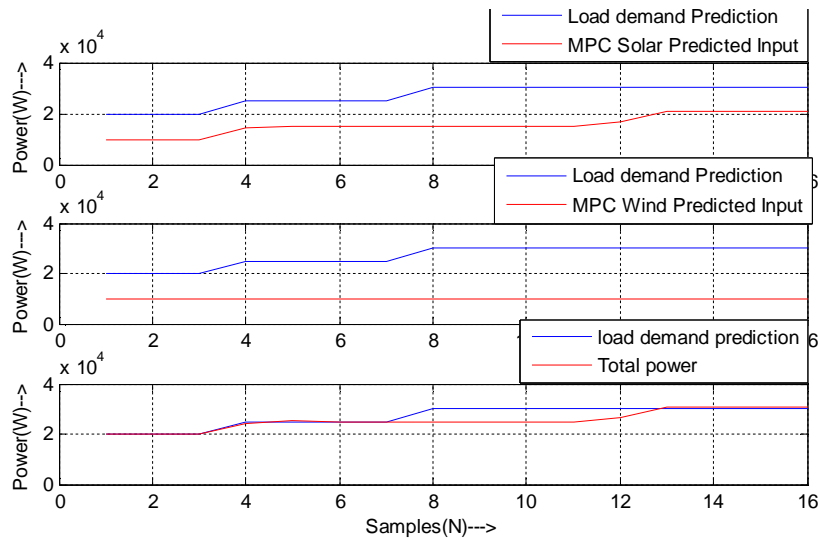


**Figure 5.7: Model predictive control implementation of HECS**

### 5.5 Conclusion

A power balancing supervisory model predictive control strategy is implemented for grid-connected HEC system. Model predictive control maintains power balance in the system based on predicted load demand. Control input  $P_{wref}$ ,  $P_{sref}$  predicted by MPC are such that their sum is always equal to the predicted load demand. Receding horizon

MPC control is implemented which proves out to be efficient, if the load predictions curve is nearly equal to the actual load demand over some period of time.

# Chapter 6

## Main Conclusions and Suggestions for further work

### **Main Conclusions:**

The major focus of this thesis has been to evolve a solar-wind hybrid energy conversion system based of model predictive control with limited power point tracking feature. The main objective was to study, design and simulate a solar wing hybrid energy conversion system with model predictive control. In order to achieve the main aim of the thesis, the system was divided into two parts, i.e. solar and wind, and then both were integrated together to get a hybrid system.

A grid-interfaced solar PV energy conversion system was designed and simulated. The system was implemented without battery at the DC-link of the grid-side converter. A sliding-mode controller based limited power point tracking algorithm was implemented and its operation was found to be satisfactory under different operating conditions. This sliding-mode controller based system was integrated with the grid using hysteresis current controller on the grid side. Mathematical modelling of the system was done and the linearized model of the system was used for model predictive control. The system with model predictive control was simulated for different operating conditions and system performance was as per expectations. The power reference given to the local controller was varying according to the demand and the power supplied by the system was following the reference given to it.

A grid-interfaced wind energy conversion system using permanent magnet synchronous generator was designed, modelled and simulated. A two-converter power electronic system was used to control the PMSG and to interface it with the grid. Hysteresis current control was used was obtaining pulses for the two converters. The outer control loop of the PMS was on a speed control loop. The speed reference for the machine was obtained using a limited power point tracking control algorithm. In order

to control the power output from the wind turbine the speed of the generator was controlled. The simulated performance of the system was verified for different operating conditions. Mathematical model of the wind energy conversion system was developed and the linearized model was used for model predictive control. Model predictive controller was the master controller and the limited power point tracking controller was the local controller. The control output of the master controller acted as the reference for the local controller. The system was simulated for different conditions of load and wind and the results were found to be satisfactory. Results verified the proper operation of both local and the master controller.

Both wind energy conversion system and the solar energy conversion system were combined at the DC-link. Model predictive controller was the master controller for both wind and solar energy conversion system and there were separate local controllers for both solar and wind. Depending upon the load demand and other operating conditions and constraints, power reference for the wind and solar energy conversion system was generated by the master controller. Depending upon the power reference, power from the wind and solar system varied. The performance of the system was verified for different operating conditions. The master controller response was satisfactory and the local controllers followed the reference signals given by the master controller.

#### **Future Work:**

- Hardware implementation of combined MPC and LPPT techniques for HECS
- Implementations of MPC and LPPT techniques for HECS standalone systems
- Implementation of MPC with solar and wind predictions, constraints on the power that can be transmitted to grid by solar and wind renewable energy sources and optimizing the operating cost of the system using appropriate cost function.
- Comparison between different control techniques used for hybrid system

---

## References

- [1] Wei Qi, Jifeng Liu, Xianzhong Chen, and Panagiotis D. Christofides. Supervisory predictive control of standalone wind/solar energy generation systems. *IEEE transaction on control system technology*, Vol. 19, No. 1, 2011
- [2] Salvador Alepuz, Sergio Busquets-Monge, Josep Bordonau. Control strategies based on symmetrical components for grid-connected converters under voltage dips. *IEEE transactions on industrial electronics*, Vol. 56, No. 6, June 2009
- [3] Trishan Eram and Patrick L. Chapman. Comparison of photovoltaic array maximum power point techniques. *IEEE transactions on energy conversion*, Vol. 22, No. 2, June 2007
- [4] F. Valenciaga, P.F. Puleston and P.E. Battaiotto. Power control of a photovoltaic array in a hybrid electric generation system using sliding mode techniques. *IEE proc-Control Theory Appl.* Vol. 148, No. 6 November 2001
- [5] Sachin Khajuria, Jaspreet Kaur. Implementation of pitch control of wind turbine using simulink. *International journal of advanced research in computer engineering & technology*. Vol. 1, Issue 4, June 2012
- [6] Mehdi Dali, Jamel Belfadj, Xavier Roboam. Hybrid solar-wind system with battery storage operating in grid-connected and stand alone mode: control and energy management-experimental investigation. *Elsevier Energy* 35(2010) 2587-2595

- 
- [7] Seul-Ki Kim, Jin-Hong Jeon, Chang-Hee Cho. Dynamic modeling and control of a grid connected hybrid generation system with versatile power system. IEEE transaction on industrial electronics, Vol. 55, No. 4, April 2008
- [8] Asraf A. Ahmed, Li Ran, Jim Bumby. Simulation and control of a hybrid PV-wind system. IEEE
- [9] Pragya Nema, R.K. Nema, Saroj Rangnekar. Renewable and sustainable energy reviews 13 (2009) 2096-2013
- [10] Remus Teodorescu, Marco Liserre and Pedro Rodriguez, Grid Converters for Photovoltaic and wind power system, Wiley: IEEE press, 2011.
- [11] T. Kawamura, K. Harada, Y. Ishihara, T. Todaka, T. Oshiro, H. Nakamura and M. Imataki, "Analysis of MPPT characteristics in photovoltaic power system", Solar Energy Materials and Solar Cells, Volume 47, Issues 1–4, October 1997, Pages 155-165, ISSN 0927-0248, 10.1016/S0927-0248(97)00036-6
- [12] Nabil A. Ahmed, A.K. Al-Othman and M.R. AlRashidi, "Development of an efficient utility interactive combined wind/photovoltaic/fuel cell power system with MPPT and DC bus voltage regulation", Electric Power Systems Research, Volume 81, Issue 5, May 2011, Pages 1096-1106, ISSN 0378-7796, 10.1016/j.epsr.2010.12.015.
- [13] S. Matsumoto, T. Shodai, Y. Kanai, "A novel strategy of a control IC for boost converter with ultra low voltage input and maximum power point tracking for single solar cell application," in Procs. Power Semiconductor Devices & IC's, 2009. ISPSD 2009. 21st International Symposium , vol., no., pp.180-183, 14-18 June 2009

---

[14] Y.P. Siwakoti, B.B. Chhetri, B. Adhikary and D. Bista, "Microcontroller based intelligent DC/DC converter to track Maximum Power Point for solar photovoltaic module," in Procs. Innovative Technologies for an Efficient and Reliable Electricity Supply (CITRES), 2010 IEEE Conference, pp.94-101, 27-29 Sept. 2010

[15] Hiroshi Kondo, Nobuyoshi Takehara, Power Converter and Electric Power Generator, US 20040027112A1

[16] Arthur F. Dickerson and Rick West, Photovoltaic DC-TO-AC Power Converter and Control Method, US 20070035975A1

[17] Khan, I. Shahidul, Md. Kashem, Abul Hoque and Md. Ariful, "Design and analysis of a mini solar grid in remote area of Bangladesh," in Procs. North American Power Symposium (NAPS), vol., no., pp.1-5, 4-6 Oct. 2009.

[18] Mukund R.Patel. Wind and Solar Power Systems: Design, Analysis, and operation.

[19] Ruisheng Li, Bingxin Wu, Xianwei Li, Fengquan Zhou and Yanbin Li , "Design of wind-solar and pumped-storage hybrid power supply system," in *Procs. Computer Science and Information Technology (ICCSIT)*, 2010 3rd IEEE International Conference on , vol.5, no., pp.402-405, 9-11 July 2010

[20] Paiva, M. S. Jose Eduardo Carvalho and S. Adriano, "An integrated hybrid power system based on renewable energy sources with electric wind MPPT," in Procs. IECON Annual Conference, pp.2981-2987, 7-10 Nov. 2010.



---

[21] S.M. Mousavi, S.H. Fathi and G.H. Riahy, "Energy management of wind/PV and battery hybrid system with consideration of memory effect in battery," in *Procs. Clean Electrical Power, International Conference*, vol., no., pp.630-633, 9-11 June 2009

[22] D.Menniti, A. Burgio, N. Sorrentino, G. Brusco An incremental conductance method with variable step size for MPPT: Design and Implementation. EPO 10<sup>th</sup> International Conference

[23] Savita Nema, R.K Nema Matlab/Simulink based study of photovoltaic cells/modules array and their experimental verification. *International Journal of Energy and Environment*. Volume 1, Issue 3, 2010

[24] Thomas Bennett, Ali Zilouchian and Roger Messenger, "Photovoltaic model and converter topology considerations for MPPT purposes", *Solar Energy*, Available online 1 May 2012, ISSN 0038-092X, 10.1016/j.solener.2012.04.005.

[25] Hung-Ching Lu and Te-Lung Shih, "Design of DC/DC Boost converter with FNN solar cell Maximum Power Point Tracking controller," in *Procs. Industrial Electronics and Applications (ICIEA), the 5th IEEE Conference*, vol., no., pp.802-807, 15-17 June 2010

[26] H.S.H. Chung, K.K. Tse, S.Y.R. Hui, C.M. Mok and M.T. Ho, "A novel maximum power point tracking technique for solar panels using a SEPIC or Cuk converter," in *Trans. Power Electronics*, vol.18, no.3, pp. 717- 724, May 2003.

---

[27] Jogendra Singh Thongman and Mohand Ouhrouche. MPPT Control Methods in wind energy conversion systems. Fundamental and Advanced topics in wind power.

[28] M.A. Abdullah, A.H.M. Yatim, C.W. Tan and R. Saidur, "A review of maximum power point tracking algorithms for wind energy systems", Renewable and Sustainable Energy Reviews, Volume 16, Issue 5, June 2012, Pages 3220-3227, ISSN 1364-0321, 10.1016/j.rser.2012.02.016

[29] Daniel, Nahum Zmood and Donald Grahame Holmes. Stationary Frame Current Regulation of PWM Inverters With Zero Steady-State Error. IEEE

[30] Adrian Timbus, Marco Liserre, , Remus Teodorescu, , Pedro Rodriguez, , and Frede Blaabjerg. Evaluation of Current Controllers for Distributed Power Generation Systems. IEEE Transactions on Power electronics, Vol. 36. March 2009

[31] Mansur Mohseni and Syed M. Islam, A new vector based Hysteresis current control scheme for three phase PWM Voltage source inverters. IEEE Transactions on Power electronics Vol. 25, No.9, September 2010

[32] Bong-hwan Kwon, Tae-Woo Kim and Jang-Hyoun Youm. A novel SVM-Based Hysteresis current control. IEEE Transactions on power electronics, Vol. 13, No. 2, March 1998

[33] Amirnaser Yazdani, Prajna paramita Dash A control methodology and characterization of dynamics for a photovoltaic system interfaced with a distribution network. IEEE Transactions on power delivery, Vol. 28, July 2009

- 
- [34] Salvador Alepuz, Sergio busquets-Monge. Control Strategies based on symmetrical components for Grid-connected converters under voltage dips. IEEE transactions on Industrial electronics, Vol. 56, No. 6, June 2009
- [35] Vladimir Lazarov, Daniel Roye, Dimitar Spirov. Study of control strategies for variable speed wind turbine under limited power conditions. 14<sup>th</sup> International Power electronics and Motion control Conference, 2010
- [36] C. Edwards and S. K. Spurgeon, Sliding mode control: theory and applications: Taylor & Francis Group, 1998
- [37] Camacho and Bordons. Model Predictive Control. Springer
- [38] J. A. Gow and C. D. Manning, "Development of a Photovoltaic Array Model for Use in Power-electronics Simulation Studies," IEEE Proceedings of Electric Power Applications, vol. 146, pp. 193-200, 1999.
- [39] F. Valenciaga, P. F. Puleston, and P. E. Battaiotto, "Power Control of a Photovoltaic Array in a Hybrid Electric Generation System Using Sliding Mode Techniques," IEE Proceedings of Control Theory and Applications, vol. 148, pp. 448-455, 2001.
- [40] H. Sira-Ramirez, "Differential geometric methods in variable structure control," International Journal of Control, vol. 48, pp. 1359-1390, 1988.
- [41] B. Singh and J. Solanki, "A comparison of control algorithms for DSTATCOM," IEEE Transactions on Industrial Electronics, vol. 56, pp. 2738-2754, 2009.

---

[42] B. Singh, P. Jayaprakash, T. R. Somayajulu, D. P. Kothari, A. Chandra, and K. Al-Haddad, "Integrated three-leg VSC with a zig-zag transformer based three-phase four-wire DSTATCOM for power quality improvement," presented at the 34th Annual Conference of the IEEE Industrial Electronics Society (IECON-2008), Florida, USA, 2008.

[43] A. K. Verma, B. Singh, and D. T. Sahani, "Grid interfaced solar photovoltaic power generating system with power quality improvement at AC mains," in 3rd IEEE International Conference on Sustainable Energy Technologies (ICSET'12), Kathmandu, Nepal, 2012.

[44] Y. Errami, M. Maaroufi, M. Ouassaid. Modelling and Control strategy of Pmsg based variable speed wind energy conversion system. IEEE

[45] Mohit Singh. Dynamic models for wind turbines and Wind power plants. NREL

[46] F.D. Kanellos, N.D. Hatziargyriou. Control of variable speed wind turbines equipped with synchronous or doubly fed induction generators supplying islanded power systems. IET Renewable power generation February 2008